

1 ClairS: a deep-learning method for long- 2 read somatic small variant calling

3
4 Zhenxian Zheng[#], Junhao Su[#], Lei Chen[#], Yan-Lam Lee, Tak-Wah Lam, Ruibang Luo*

5
6 Department of Computer Science, The University of Hong Kong, Hong Kong, China

7
8 [#] These authors contributed equally to this work

9 * To whom correspondence should be addressed. Email: rbluo@cs.hku.hk

12 Abstract

13 Identifying somatic variants in tumor samples is a crucial task, which is often performed using
14 statistical methods and heuristic filters applied to short-read data. However, with the increasing
15 demand for long-read somatic variant calling, existing methods have fallen short. To address this
16 gap, we present ClairS, the first deep-learning-based, long-read somatic small variant caller.
17 ClairS was trained on massive synthetic somatic variants with diverse coverages and variant
18 allele frequencies (VAF), enabling it to accurately detect a wide range of somatic variants from
19 paired tumor and normal samples. We evaluated ClairS using the latest Nanopore Q20+
20 HCC1395-HCC1395BL dataset. With 50-fold/25-fold tumor/normal, ClairS achieved a
21 93.01%/86.86% precision/recall rate for Single Nucleotide Variation (SNVs), and 66.54%/66.89%
22 for somatic insertions and deletions (Indels). Applying ClairS to short-read datasets from
23 multiple sources showed comparable or better performance than Strelka2 and Mutect2. Our
24 findings suggest that improved read phasing enabled by long-read sequencing is key to accurate
25 long-read SNV calling, especially for variants with low VAF. Through experiments across various
26 coverage, purity, and contamination settings, we demonstrated that ClairS is a reliable somatic
27 variant caller. ClairS is open-source at <https://github.com/HKU-BAL/ClairS>.

30 Introduction

31 Analysis of cancer genomes that identify and characterize somatic variants has enabled a better
32 understanding of tumor progression¹ and led to precision oncology². Identifying somatic
33 variants, however, remains challenging due to intra- and inter-tumor heterogeneity, which often
34 leads to low VAF, and confounding factors, including sequencing artifacts, inadequate
35 sequencing coverage, and normal contamination³. Endeavors were made to address these
36 challenges and maximize sensitivity and accuracy in identifying somatic variants using next-
37 generation sequencing (NGS) short-reads⁴⁻¹³. However, constrained by read length, short reads

38 have limited variant discovery capability in hard-to-map genomic regions, such as
39 homopolymers and segmental duplications. This problem is expected to be alleviated through
40 long-read sequencing¹⁴. Oxford Nanopore Technologies (ONT) is among the leading long-read
41 sequencing technologies and offers miniaturized sequencing devices and fast sample-to-data
42 turnaround, which is a credible step towards democratizing sequencing by drastically reducing
43 the cost of carrying out sequencing experiments. ONT raw reads were reported to have an error
44 rate of 3-15% in the past¹⁵. This was reduced to 1% or lower using ONT's latest Q20+
45 chemistry¹⁶. The gap is still significant, however, compared with NGS short-reads, which have an
46 average error rate at 0.1%¹⁷, making the somatic variant callers once designed for short reads
47 practically unworkable for ONT long-reads.

48
49 Germline variants are often considered to be easier to correctly identify than somatic variant
50 calling. The first attempt to call germline small variants using noisy ONT long-reads was made by
51 Clairvoyante in 2018¹⁸. The work was enabled using 1) a deep neural network, which was first
52 used for variant calling by DeepVariant¹⁹; and 2) the high-quality known truth variants in GIAB
53 reference samples for neural network model training²⁰. Subsequent works by Clairvoyante
54 including Clair²¹ and Clair3²², introduced optimized network input, network output, network
55 architecture, and workflow designs to make the best out of noisy ONT data for germline small
56 variant calling. Both Clair3 and a pipeline named PEPPER-Margin-DeepVariant²³ (DeepVariant),
57 which is also designed for ONT long-read germline small-variant calling, have demonstrated
58 better single nucleotide polymorphism (SNP)-calling performance than using the same coverage
59 of Illumina short reads. However, while solutions are ready for ONT long-read germline small-
60 variant calling, there has been no caller available for ONT long-read somatic small-variant
61 calling. We note that ONT long-read somatic SV (structural variant) callers, including Sniffles2²⁴
62 and Nanomonsv²⁵, which were developed in the past year called for the development of a small
63 variant caller to complete the ONT long-read somatic variant-calling workflow.

64
65 Unfortunately, some designs critical to ONT long-read germline variant calling are not applicable
66 to somatic variant calling. First, in their network output, both Clair3 and DeepVariant apply a
67 strong diploid genome assumption. Clair3 uses a 21-genotype output, which is a two-
68 combination of A, C, G, T, insertion, and deletion²². DeepVariant uses a three-category output
69 that includes hom-ref (homozygous reference), het (heterozygous), and hom-alt (homozygous
70 alternative)²³. Both Clair3 and DeepVariant are classification models that use observed allele
71 frequency of alternative alleles as network input, and output the category that represents the
72 expected allele frequency of a variant (e.g., allele frequency 0, 0.5, 1, and 0.5/0.5 for genotype
73 0/0, 0/1, 1/1, and 1/2, respectively). However, somatic variants have VAF ranging continuously
74 from 0 to 1. Without a certain ploidy, somatic variant candidates have no expected allele
75 frequency for a model to test against. Thus, a new design is required. As an example, a new
76 design could use a regression model to derive VAF directly, or a classification model to simply
77 determine whether a candidate is a somatic variant or not and infer VAF subsequently. Second,
78 the seven standard GIAB reference samples HG001–HG007 provide approximately 25 million
79 truth germline variants²⁰, which are critical for the model training of any state-of-the-art, deep-
80 learning-based germline variant callers. However, in terms of known truth somatic variants, only
81 the HCC1395–HCC1395BL (a human triple-negative breast cancer cell line and a normal cell line

82 derived from the B lymphocytes of the same donor, hereafter referred to as HCC1395/BL
83 tumor-normal pair was published by the Somatic Mutation Working Group of the SEQC2
84 (Sequencing Quality Control Phase II) consortium³. It contains only 39,560 SNVs and 1,922
85 Indels, which is orders of magnitude fewer than the available truth germline variants, and far
86 from enough for deep neural-network model training. In the absence of adequate real tumor-
87 normal samples, one could think of synthetic data as a solution. Bamsurgeon spiked somatic
88 variants into sequencing reads to mimic a tumor²⁶. This was a successful method for short
89 reads, but it doesn't work for long reads for two reasons: 1) Illumina short reads are read one
90 base at a time, whereas ONT long reads are read as the signals of a sliding 5-mer or 6-mer
91 window. That is, a spike-in variant also changes the signals of the adjacent bases. Bases can be
92 base-called from signals but cannot be authentically turned back into signals, so the spike-in
93 method cannot be applied to long reads; and 2) Bamsurgeon does not apply the point that a
94 somatic variant is usually found in only one haplotype (either maternal or paternal) but is
95 missing in another. The use of long reads over short reads for somatic variant calling makes
96 sense only if the long-read advantage of haplotyping (also called phasing) is utilized. All things
97 considered, a new method for synthesizing long-read data to contain abundant plausible
98 somatic variants is needed.

99
100 In this study, we present Clair-Somatic (ClairS), the first somatic small variant caller for ONT long
101 reads, which is named after its germline variant caller predecessors. ClairS draws on the
102 successful experience of the Clair series, and uses a new network output and a new workflow
103 design to address the continuous VAF space of somatic variants. By considering two different
104 samples, A and B, as tumor and normal, respectively, and deeming a germline variant specific to
105 A as a somatic variant against B, we devised a data synthetic strategy that uses only the real
106 long reads of GIAB reference samples with known germline variants, but can simulate somatic
107 variants of any tumor purity, sequencing coverage (lower than the data source), and level of
108 normal contamination. The strategy can theoretically produce an infinite number of somatic
109 variants for model training. We show results to highlight how phasing improves somatic variant-
110 calling performance on long reads. To leverage more remote alignment information that is
111 computationally impractical to include in the network input, we devised a post-processing step
112 that searches for ancestral haplotype support for any somatic variant candidates. This step
113 removed a considerable amount of false positive calls in our experiments. For benchmarking,
114 we sequenced in total 75-fold HCC1395 and 45-fold HCC1395BL ONT Q20+ long-reads (data
115 deposited to NCBI SRA), and used the truth somatic variants provided by the SEQC2
116 consortium³. With 50-fold/25-fold tumor/normal, ClairS achieved 86.86%/93.01%
117 recall/precision rate SNVs, and 66.89%/66.54% for somatic Indels when targeting VAF ≥ 0.05 . For
118 variants with VAF ≥ 0.2 , the numbers go up to 94.65%/96.63% for SNVs, and 73.22%/77.35% for
119 somatic Indels. We also show the performance of ClairS at different tumor/normal coverages,
120 tumor purity and normal contamination. ClairS is designed for ONT long reads, but the whole
121 method is also applicable to Illumina short reads. This versatility allowed us to benchmark ClairS
122 against state-of-the-art short-read somatic variant callers considering that there is no other
123 long-read somatic variant caller to benchmark against. The results show that ClairS performed
124 comparably or slightly better than the current heuristic-based and deep-learning-based callers
125 on short reads.

126
127

128 Results

129 The ClairS method

130 The ClairS method is elaborated in the Method section. Texts in **bold** in this and the following
131 two paragraphs can be found as subsection titles in the Method section. In the use of deep-
132 learning for long-read somatic variant calling, ClairS has made breakthroughs in **Training data**
133 **synthesis** and the **ClairS workflow and design**.

134

135 Regarding training data synthesis, Figure 1a shows the workflow for **Generating synthetic tumor**
136 **and synthetic normal**. As we required sampling without replacement, and in view of the
137 common practice that a tumor sample having higher coverage than its matching normal, we
138 gave **Coverage advice for the source data**. Details of how homozygous and heterozygous
139 germline variants in different samples are converted into somatic variants are given in **Deriving**
140 **multiple categories of variants from a synthetic tumor/normal pair**. Setups to avoid practical
141 concerns and limitations of the data synthesis method are given in **Other details about the**
142 **variants selected for model training**. Our data synthesis method is based on the observation
143 that an authentic somatic variant is usually found in the reads of a single haplotype (depicted in
144 Extended Data Figure 1a). Also, we found that **Phasing information enhances somatic variant**
145 **calling performance** in ClairS.

146

147 Regarding the ClairS workflow and design, Figure 2a shows an **Overview** of the ClairS workflow.
148 Figure 2b shows **Step 1: Germline variant calling, phasing and read haplotagging**, and Figure 2c
149 shows **Step 2. Pileup-based and full-alignment based variant calling**. For each sample, while
150 only a fraction of genome positions has alternative allele support and among them, only a few
151 have the potential to be called somatic variants, we used heuristics for **Selecting variant**
152 **candidates**. Details of **The design of pileup input and full-alignment input** and **The design of**
153 **neural networks** are shown in Figure 3. The ways in which ClairS differs from its predecessor,
154 Clair3, are discussed in Method. Figure 2d shows **Step 3. Search for ancestral haplotype**
155 **support**, which is a post-processing step that leverages more remote alignment information to
156 search for ancestral haplotype support to the somatic variants called in step 2. To adapt to
157 different usage scenarios, multiple **Output** options are provided.

158

159 ClairS performance on ONT data

160 A summary of the ONT data used for model training and benchmarking is shown in
161 Supplementary Table 1. We trained the ClairS ONT model using synthetic data generated from
162 two GIAB samples: HG001 and HG002²⁰. We used both HG001/HG002 and HG002/HG001 as
163 tumor/normal samples for data synthesis. The HG002 sample has 76.29-fold coverage and was
164 made available by Nanopore through EPI2ME Labs. The HG001 sample has 48.44-fold coverage
165 and was sequenced at HKU, with details given in the Method – ONT library preparation and

166 sequencing section. Following the convention of the state-of-the-art deep-learning-based
167 variant callers, we excluded reads and variants from Chromosome 20 from model training.
168
169 For benchmarking, we used the HCC1395/BL tumor-normal pair, with known truth variants
170 provided by the SEQC2 consortium³. The HCC1395 sample has 75.97-fold coverage. The
171 HCC1395BL sample has 45.55-fold coverage. Both samples were sequenced at two sequencing
172 centers (HKU and Novogene) for quality control purposes. The yield of the two centers is shown
173 in Supplementary Table 2. Only SEQC2 truth variants labeled “HighConf” (high confidence) and
174 “MedConf” (medium confidence) were used for benchmarking. While there are ~40k SNVs but
175 only ~2k Indels in the truth set, the big difference in the number of truth variants results in
176 different analytical power between the two variant types. So we first benchmarked multiple
177 coverages, tumor purity and normal contamination with only SNVs, and then benchmarked and
178 discuss somatic Indel-calling performance in a separate section. We used Illumina’s Haplotype
179 Comparison Tools²⁷ to generate the performance figures, including F1-Score, Precision, and
180 Recall, and cross-validated them with the “compare_vcf” submodule in ClairS. More
181 clarifications and parameters are shown in the Method – Benchmarking section.
182
183 For both model training and benchmarking, we used GRCh38, which is the newest reference
184 genome version on which both GIAB and SEQC2 truth variants are based. All ONT sequencing
185 data were base-called using Guppy version 6.1.5 and aligned to GRCh38 using minimap2 version
186 2.17-r941. The command line used is given in the Supplementary Notes – Command lines used
187 section. All data mentioned above, including ONT sequencing data, GIAB truth variants, SEQC2
188 truth variants, and reference genomes, are publicly accessible via links or SRA accession IDs
189 listed in the Supplementary Notes – Data availability section.
190
191 *Performance with different tumor combinations and normal coverage.* We assessed the ClairS
192 performance with different combinations of tumors and normal coverage. We tested three
193 tumor coverage rates: 25-, 50-, and 75-fold. We applied 25-fold as the first step as it represents
194 a conservative throughput estimation of an R10.4.1 PromethION flowcell. We also tested three
195 normal coverages: 20-, 25-, and 30-fold. The 25-fold step resembles the throughput variance of
196 a single flowcell. Our experiments aimed to imitate a practical setting for clinical cancer
197 diagnosis, with the tumor sample coverage increased one flowcell at a time to seek higher
198 discovery power, but the normal sample coverage is fixed at a single flowcell for cost-
199 effectiveness.
200
201 The results are shown as Precision-Recall curves in Figure 4a. The evaluation metrics at two
202 variant quality cutoffs (8 and 15) are shown in Supplementary Table 3. Quality cutoff 15
203 (hereafter referred to as “prioritize-f1 mode”) filters more variants and aims for balanced
204 precision and recall. Quality cutoff 8 (“prioritize-recall mode”) retains more variants and aims
205 for higher recall. In the prioritize-f1 mode, with normal coverage fixed at 25-fold, ClairS achieved
206 95.03%/78.71%/86.11%, 93.01%/86.86%/89.83%, and 92.94%/86.92%/89.83%
207 precision/recall/f1-score at 25-, 50-, and 75-fold tumor coverage, respectively. From 25- to 50-
208 fold, the recall increased from 78.11% to 86.86% (+8.75%), with a 2.02% precision drop (from
209 95.03% to 93.01%). From 50- to 75-fold, however, no improvement was observed. In the

210 prioritize-recall mode, also with normal coverage fixed at 25-fold, ClairS achieved
211 82.66%/91.55%/86.88%, 70.21%/96.10%/81.14%, and 63.80%/96.60%/76.85%
212 precision/recall/f1-score at 25-, 50-, and 75-fold tumor coverage, respectively. Compared to
213 prioritize-f1, the prioritize-recall mode reached 91.55% recall at 25-fold (against 78.71%,
214 +12.84%), and 96.10% at 50-fold (against 86.86%, +9.24%). Although Clair3 is not designed for
215 somatic variants, to give a reference point, we conducted experiments with it using the same
216 datasets by considering the germline variants found in tumor but not in normal as somatic
217 variants. At 25-fold normal, Clair3 had a 19.27%/72.10%/30.42%, 29.82%/68.32%/41.52%, and
218 36.21%/64.56%/46.40% precision/recall/f1-score at 25-, 50-, and 75-fold tumor coverage. The
219 results highlight the inappropriateness of using a germline variant caller for somatic variant
220 calling.

221
222 In both prioritize-f1 and prioritize-recall modes, raising the normal coverage consistently
223 increased somatic variant-calling performance. With tumor coverage fixed at 50-fold and using
224 the prioritize-f1 mode, ClairS achieved a 91.86%/83.77%/87.63%, 93.01%/86.86%/89.83%, and
225 92.06%/88.51%/90.25% precision/recall/f1-score at 20-, 25-, and 30-fold normal coverage. The
226 numbers were 68.36%/95.69%/79.75%, 70.21%/96.10%/81.14%, and 70.56%/96.43%/81.49%
227 in the prioritize-recall mode.

228
229 Figure 4b shows the performance of ClairS in prioritize-recall mode, broken down to four VAF
230 ranges: 0.5-1, 0.2-0.5, 0.1-0.2, and 0.05-0.1. At different coverages, the performance of ClairS at
231 range 0.2-0.5 (low-mid) was found to be as good as 0.5-1 (mid-high). For example, at 50/25-fold
232 tumor/normal coverage, ClairS achieved a 94.7%/99.3%/96.9% precision/recall/f1-score at 0.5-
233 1, and 95.2%/98.1%/96.7% at 0.2-0.5. At range 0.1-0.2, precision was reduced to ~60%, while
234 recalls plateaued at ~90%. At range 0.05-0.1, precision was further reduced to below 10%
235 (11.8%, 5.7%, and 4.6% at 25-, 50-, and 75-fold tumor coverage), while recalls were raised with
236 increasing tumor coverage (16.5%, 32.8%, and 46.1%). The reason for the drop in precision was
237 that the higher coverage led to a drastic increase in the number of variant candidates at very
238 low VAF. At range 0.05-0.1, the number of candidates was about 131k, 310k, and 419k at 25-,
239 50-, and 75-fold tumor coverage.

240
241 *Performance at different tumor purities and normal contamination.* We assessed the
242 performance of ClairS at different combinations of tumor purity (1.0, 0.8, 0.6, 0.4, and 0.2) and
243 normal purity (1.0, 0.95, and 0.90). All the experiments in this section used 50-fold tumor and
244 25-fold normal coverage. The results are shown in Figure 4c and Supplementary Table 4. The
245 two modes (prioritize-f1 and prioritize-recall) behaved differently with varying purity. With
246 normal purity fixed at 1.0, in prioritize-f1 mode, precision remained above 90% (93.01%,
247 96.25%, 97.79%, 98.68%, and 98.99% at tumor purity 1.0, 0.8, 0.6, 0.4, and 0.2), while recall
248 dropped (86.86%, 81.63%, 71.08%, 52.94%, and 22.43%) with decreasing tumor purity. In the
249 prioritize-recall model, precision varied (70.21%, 80.11%, 88.14%, 93.81%, and 97.54%), while
250 recall was boosted, especially at lower tumor purity (96.10%, 94.45%, 90.51%, 80.81%, and
251 53.06%). According to these results, generally, we suggest using prioritize-f1 mode at higher
252 tumor purity and prioritize-recall mode at lower tumor purity.

253

254 Our results also showed that lower normal purity harmed somatic variant-calling performance,
255 especially on recall. With tumor purity fixed at 1.0, in prioritize-f1 mode, the recalls were
256 86.86%, 70.35%, and 51.74% at normal purity 1.0, 0.95, and 0.90. In prioritize-recall mode, the
257 recalls were 96.10%, 85.36%, and 69.42%. Accordingly, we suggest using a high-purity normal
258 sample with ClairS for somatic variant discovery. Lastly, we showed the results using 0.8/0.95
259 tumor/normal purity. In prioritize-recall mode, ClairS achieved a 79.68%/81.13%/80.40%
260 precision/recall/f1-score, demonstrating ClairS' reliability in challenging sample conditions.
261

262 *Analysis of False Positive and False Negative calls.* Using 50-fold tumor and 25-fold normal
263 coverage, we manually analyzed 300 false positive and 300 false negative calls randomly picked
264 from all variant calls. Each FP and FN was assigned with the most obvious limitation as the
265 reason why the call was false. The reasons for the 600 false calls are listed in Supplementary
266 Table 5. A distribution of the reasons is given in Figure 4 as a pie chart.
267

268 Among the false positive calls, 39% had no matching truth but were with tumor $0.05 \leq VAF < 0.1$,
269 22% were with tumor $0.1 \leq VAF < 0.15$, and 9% were with tumor $VAF \geq 0.15$. As the Method section
270 elaborates, these calls are with tumor and normal coverage ≥ 4 , and normal VAF below 0.05.
271 One possible explanation is that ClairS was unable to pick up more hints and tell these calls from
272 the true ones. Some of these cases might be correctly called again with higher tumor coverage,
273 which reduces the statistical bias in VAF. It is also possible that since the SEQC2 truth set is still
274 under active development, its incompleteness caused a few variants that are actually true to be
275 misclassified as false positives. Another major category of false positive calls is likely to be
276 caused by alignment artifacts because of a repetitive or imperfect genome reference sequence.
277 It includes 6% “One or more deletions in flanking 50bp”, 5% “In low complexity region”, 4%
278 “Excessive mismatches in alignment”, 3% “One or more insertions in flanking 50bp”, and in
279 total, another 10% in repetitive regions of different types. Also, we found 1% false positive calls,
280 possibly because of insufficient normal coverage.
281

282 Among the false negative calls, 40% truth variants that were not called were with tumor
283 $VAF < 0.1$, 10% were with “Normal VAF ≥ 0.05 , but tumor VAF < 6 times larger than normal VAF”,
284 and 3% were with < 3 reads supporting the variant allele in a tumor. These missed variants might
285 be called again if higher tumor coverage is given. False negative calls are more likely to be
286 caused by alignment artifacts, as we observed 10% false negative calls in the homopolymer
287 region, 10% in the low complexity region, 7% in the tandem repeat region, and in total, another
288 9% that were also likely to have been caused by alignment. We also observed 4% false negative
289 calls caused by extreme strand bias (i.e., reads observed in only one strand); and 1% with base
290 quality of all supporting bases < 20 .
291

292 *Somatic Indel-calling performance.* The SEQC2 truth set provides ~40k SNVs but only ~2k Indels.
293 Owing to the scarcity of truth somatic Indels that could reduce statistical biases, we
294 benchmarked somatic Indel-calling separately. The results of different combinations of tumor
295 coverage (25-, 50-, and 75-fold) and normal coverage (20-, 25-, and 30-fold) are shown in
296 Supplementary Table 6. With normal coverage fixed at 25-fold, in prioritize-f1 mode (variant
297 quality cutoff at 12) ClairS achieved 76.91%/49.36%/60.13%, 66.54%/66.89%/66.72%, and

298 57.79%/71.48%/63.91% of precision/recall/f1-score at 25-, 50-, and 75-fold tumor coverage. In
299 prioritize-recall mode (cutoff at 8), ClairS achieved 53.05%/65.46%/58.61%,
300 38.63%/76.15%/51.25%, and 37.55%/76.60%/50.40%. As in our conclusion for SNV calling,
301 generally, we suggest using prioritize-recall mode for calling somatic Indels at lower tumor
302 coverage.

303

304 *Performance after adding phasing information to the input in step 2.* The reconstruction of
305 haplotypes, also known as haplotype-resolved assembly or phasing, greatly improved the
306 performance of long-read germline variant calling in previous practice^{22,23}. In the Method
307 section, we elaborate how phasing information can be used to enhance somatic variant-calling
308 performance. Using 50/25-fold HCC1395/BL and prioritize-recall mode for benchmarking, we
309 show in Extended Figure 1b that phasable somatic variants performed better than unphasable
310 ones, especially at lower VAF. At VAF 0.1-0.15, phasable somatic variants had a
311 43.8%/85.6%/57.9% precision/recall/f1-score, but unphasable somatic variants had only
312 16.4%/81.2%/27.3%. At VAF 0.05-0.1, phasable somatic variants had 5.8%/46.6%/10.3%, but
313 unphasable somatic variants had only 2.3%/27.2%/4.3%. We tried disabling phasing in ClairS
314 and fed no phasing information to the calling networks. As shown in Supplementary Table 7, the
315 overall F1-score dropped from 81.14% to 78.66% (-2.48%).

316

317 *Performance of the two respective networks in step 2.* In contrast to Clair3, in which the pileup
318 network handles all the variant candidates, and the full-alignment network processes only the
319 undecided candidates using the pileup network, ClairS uses both networks equally to make
320 collective decisions. The rationale and details are elaborated in the Method section. We tested
321 the performance using both the pileup network only and the full-alignment network only, with
322 50/25-fold of HCC1395/BL and prioritize-recall mode. The results are shown in Supplementary
323 Table 7. When we used only the pileup network, the F1-score dropped from 81.14% to 73.27%
324 (-7.87%). When we used only the full-alignment network, the F1-score dropped from 81.14% to
325 79.14% (-2.00%).

326

327 *Performance of Step3: Searching for ancestral haplotype support.* As elaborated in the Method
328 section, step 3 utilizes remote alignment signals that could not be included in the network
329 inputs due to computational limitations to improve the precision of the called somatic variants.
330 As shown in Supplementary Table 7, without this step, the precision dropped from 70.21% to
331 67.14% (-3.07%, using 50/25-fold HCC1395/BL and prioritize-recall mode).

332

333 ClairS performance on Illumina data

334 Short-read somatic small-variant calling has been intensively studied. A non-exhaustive list of
335 state-of-the-art methods include Strelka2¹⁰, Mutect2⁸, Lancet⁶, Neusomatic⁵, Octopus¹²,
336 SomaticSniper⁹, and Varnet⁴. ClairS was designed primarily for long-read somatic small-variant
337 calling. However, it poses no limitations to small reads, and we expect a variant-calling method
338 that works for long reads to perform as well as or even better than existing short-read methods.
339 Also, benchmarking against other short-read somatic small-variant callers provides insights on

340 how ClairS performs against existing methods, since no other long-read callers are available for
341 comparison.

342

343 A summary of the Illumina data used for model training and benchmarking is shown in
344 Supplementary Table 1. We used both HG003/HG004 and HG004/HG003 as tumor/normal
345 samples for data synthesis. The HG003 and HG004 samples had 91.15- and 88.49-fold coverage,
346 and were publicly shared by Google Health Center. For benchmarking, we also used the
347 HCC1395/BL tumor-normal pair, but with data from six sequencing centers, made available by
348 the SEQC2 consortium – NS: NovaSeq at Illumina; NC: HiSeq at the National Cancer Institute, IL;
349 HiSeq at Illumina, EA; HiSeq at European Infrastructure for Translational Medicine, FD; HiSeq at
350 Fudan University, NV; HiSeq at Novartis – with coverage ranging from 37.93- to 87.54-fold. The
351 six multi-center replicates enabled us to verify ClairS' performance consistency. If not
352 specifically mentioned, other training and benchmarking details are the same as those of the
353 ONT data experiments, and we benchmarked only SNVs for all callers. Like the ONT data
354 experiments, the command lines and links to the data used for both model training and
355 benchmarking are listed in the Supplementary Notes.

356

357 The evaluation metrics of the eight callers on the six datasets are shown in Supplementary Table
358 8. Figure 6a shows the precision-recall curves, and figure 6b shows a histogram of the F1-scores.
359 ClairS consistently performed comparably or slightly better than the two top-performing callers,
360 Strelka2 and Mutect2. On the six datasets, ClairS achieved a 97.88%, 97.82%, 97.46%, 97.53%,
361 97.03%, and 96.41% F1-score. Strelka2 achieved a 96.16%, 96.18%, 97.03%, 97.35%, 96.32%,
362 and 95.47%. Mutect2 achieved 95.21%, 95.75%, 95.33%, 96.24%, 96.46%, and 94.35%. Broken
363 down into different VAF ranges, the ClairS performance was also consistently comparable to or
364 better than that of other callers, as shown in Figure 6c. Figure 6d shows Venn diagrams of the
365 overlaps of false positive calls between Strelka2, Mutect2, and ClairS. The diagrams show that
366 although rare, there are 30 to 41 false positive calls in the six datasets that were called by all
367 three callers. Owing to the possible incompleteness of the truth set, a false positive variant can
368 be either a wrong call or a true variant missing from the truth set. These false positive variant
369 calls called by all three callers are worth conducting further verification and might further
370 contribute to the completeness of the truth set.

371

372 Discussion

373 In this study, we present ClairS, the first somatic small variant caller for ONT long-reads. In our
374 benchmarks, we showed that it is reliable at different sample coverages, tumor purities and
375 normal contaminations. With the training data synthesis method we devised, ClairS can be
376 trained for somatic small-variant calling for any sequencing platform. We demonstrated that
377 ClairS performed as well as or even better than the top-performing somatic variant callers for
378 Illumina short reads. ClairS draws on its germline variant caller predecessors' experience, while
379 using a redesigned workflow, network architecture, network output, and post-processing
380 procedure for the more challenging somatic variant-calling tasks.

381

382 The use of long reads for somatic SV discovery has unraveled complex somatic SVs that were
383 previous hampered by short reads²⁸. With the unprecedented power of long reads to cover
384 repetitive genome regions, we expect the use of long reads for somatic small variant calling to
385 reveal more somatic variants that were previously inaccessible by short reads, and lead to a
386 better understanding of the mutational processes and functional consequences of the somatic
387 variants in different cancer types. To allow more researchers to achieve these goals, ClairS was
388 included as the small variant caller in ONT's somatic variant-calling workflow²⁹.
389

390 Despite using ONT's latest Q20+ data, the F1-score for somatic indels was only ~60%. Although
391 the performance looks better when considering only the somatic indels in the coding
392 sequences, the promise of better whole genome somatic indel-calling performance lies in the
393 continuous advancement of ONT's sequencing chemistry and base-calling algorithm.
394

395 Method

396 Training data synthesis

397 *Generating synthetic tumors and synthetic normal.* A tumor comprises normal cells and tumor
398 cells; the latter are regarded as foreign. Similarly, the normal cells of an individual are
399 considered foreign to the normal cells of another individual, and vice versa. The germline
400 variants unique to an individual can mimic a somatic variant when mixed with another
401 individual. With insufficient known truth somatic variants and standard tumor-normal sample
402 pairs available, this observation lays the foundation for generating ample synthetic somatic
403 variants from known truth germline variants in the GIAB reference samples with real
404 sequencing data for deep-learning model training. The detailed workflow is shown in Figure 1a.
405 Using 80-fold GIAB HG002 of ONT WGS alignments as the source of the tumor (hereafter
406 referred to as A) and 50-fold of HG001 as the source of normal (B) as an example, we first split
407 the alignments of both samples into smaller chunks, each with 4-fold coverage. The smaller
408 chunks from both samples can be combined to simulate 1) different allele frequencies, such as
409 combining 40-fold A, i.e., 10 4-fold chunks of A with 20-fold B, i.e., 5 4-fold chunks of B, to
410 simulate a synthetic tumor sample with an ideal 67% allele frequency, i.e., 40-fold of A against
411 60-fold of A+B; 2) different coverage of both tumor and normal, e.g. increase or decrease the
412 number of chunks as needed; and 3) different levels of contamination in normal, e.g., instead of
413 using 100% A as normal, adding one or more chunks of B in normal.
414

415 *Coverage advice for the source data.* We applied two restrictions to tumor and normal
416 synthesis. First, to avoid any biases caused by reusing individual reads, we used sampling
417 without replacement in tumor and normal synthesis. That is, a chunk that was used could not
418 be used again. Second, we required the synthetic tumor to have equal or higher coverage than
419 the synthetic normal to align with common practice. Using the previous example, i.e., 80-fold A
420 as the source of a tumor, and 50-fold B as the source of normal, if 20-fold B is reserved to mix
421 with A for the tumor, then 30-fold B is left for normal, but we can achieve tumor purity only
422 between 33% (10-fold A + 20-fold B) and 100% (80-fold A + no B). However, if 30-fold B is

423 reserved to mix with A for the tumor, tumor purity between 0% (no A + 30-fold B) and 100%
424 (80-fold A + no B) can be achieved, but only 20-fold B is left for normal. Thus, we suggest using
425 the sample with higher coverage as the source of normal to achieve both higher normal
426 coverage and full-spectrum tumor purity for model training. This is counterintuitive because
427 higher tumor coverage of common in cancer studies.
428

429 *Deriving multiple categories of variants from a synthetic tumor/normal pair.* Four categories of
430 variants, namely “Somatic”, “Germline”, “Artifact”, and “Normal-only”, were derived from a
431 synthetic tumor/normal pair, as explained in detail in Figure 1a. We used GIAB truth variants in
432 the synthetic tumor and synthetic normal, and we defined any truth variants (including both
433 homozygous and heterozygous) as “callable-variant”. Basically, somatic variants are callable
434 variants in the synthetic tumor but not in the synthetic normal, which are also known as truth
435 germline variants in the tumor source, but not in the normal source. Germline variants are
436 callable variants in both the synthetic tumor and synthetic normal, which are also known as
437 truth germline variants in both the tumor source and normal source. Artifact variants are
438 callable variants only in the synthetic tumor. They are not known as truth in either the tumor
439 source or the normal source. Normal-only variants are callable-variants found only in the
440 synthetic normal. Three of the four categories, Somatic, Germline and Artifact, are used for
441 model training. Only the variants located in the overlapping GIAB-defined high-confidence
442 regions of both the tumor and normal sources were used for training to ensure the quality of
443 the training variants. Because of the sub-sampling process, some variants might have few
444 supporting reads in the synthetic tumor, especially for low AF somatic variants. These variants
445 were excluded from model training to avoid confusing the neural network. More exclusion
446 details are given in the following paragraph. Our sample synthesis method supports generating
447 synthetic tumors at any purity level, so we can use as many purities as possible to achieve fine
448 coverage of VAF from 0 to 1, but for practicality, we used three tumor purities (25%, 50%, and
449 100%), and applied subsampling to all variants from the three purities to achieve acceptable
450 VAF distribution. This is feasible because 1) the innate variance of the AF of the germline
451 variants from the tumor and normal sources enables a pool of somatic variants fully covering
452 VAF from 0 to 1, even with just three purities, and 2) applying subsampling to the pool enables
453 us to enrich difficult somatic variants and reduce the number of less common somatic variants
454 for model training. In terms of subsampling, the VAFs of chosen somatic variants were randomly
455 selected from a beta distribution with shape parameters $\alpha=2$ and $\beta=5$. The same distribution
456 was used by the SEQC2 consortium for spike-in somatic variants in Sahraeian et al³⁰. Our
457 experiment showed that subsampling itself resulted in a ~1.8% increase in the F1-score using
458 50x/25x of HCC1395/BL. The resulting VAF distribution of SNVs is shown in Figure 1b. We tried
459 adding one more tumor purity at 12.5%, but apart from longer model training time, no
460 performance gain was observed.
461

462 *Other details about the variants selected for model training.* For the somatic variants used for
463 model training, a minimum coverage of four, and a minimum of three reads supporting the
464 somatic variant allele are required. Somatic variants with $VAF > 0.03$ in the synthetic normal
465 were excluded from training to avoid confusing the model with a very noisy normal. For the
466 artifacts, the non-reference AF was capped at 0.05 to avoid using a large number of obvious

467 artifacts for training. For germline variants, minimum coverage of four reads and a minimum of
468 three reads supporting the germline variant allele, were required in both synthetic tumor and
469 normal. Germline variants with a difference in AF larger than 0.1 between the synthetic tumor
470 and normal were excluded from training. To prevent the model from inferring a somatic variant
471 from its co-existence with two or more adjacent germline variants, which is a confounding
472 factor that can be easily learned by the model, germline variants that were less than 33bp (the
473 window size of our model design) from each other were excluded from training. Our experiment
474 showed that this exclusion alone increased somatic variant calling precision by ~1%. With three
475 tumor purities and the exclusions explained above, 12,489,342 training samples were left. The
476 breakdown is shown in Figure 1c.

477

478 *Phasing information enhances somatic variant-calling performance.* An authentic somatic
479 variant usually originates from either the maternal or paternal haplotypes, while a random error
480 usually has a fair chance happening in both (Extended Data Figure 1a). Thus, somatic variants
481 that have a single ancestral haplotype (either maternal or paternal) should be considered more
482 reliable than those with two ancestral haplotypes, except for somatic variants with high VAF
483 that might be a result of copy number alteration or clonal duplication³¹. ClairS uses phasing
484 information for both model training and inference. Clair3 and LongPhase are used for phasing
485 and read haplotagging. More details are given in the “ClairS input and output” section. ClairS
486 uses phasing information during full-alignment-based variant calling, in which a channel named
487 “Tumor/Normal/Phasing Info” is used. In this channel, the alignments are grouped into
488 haplotype-unknown, haplotype 1, and haplotype 2, each using the read order of the
489 alignments. Although long-read sequencing enables outstanding phasing performance, some
490 somatic variants in difficult genomic regions or without a heterozygous germline in their vicinity
491 still cannot be covered by any phased reads. Thus, during model training, for each variant that
492 has a heterozygous origin from the tumor source, if one or more reads can be phased, both a
493 version of input with reads after phasing and a version before phasing were used.

494

495 **ClairS workflow and design**

496 *Overview.* Figure 2 shows an overview of the ClairS somatic variant-calling workflow. Starting
497 from the alignments in the BAM/CRAM format of a tumor/normal sample pair, ClairS follows
498 three steps to derive the somatic variants in a tumor and outputs them to a VCF file. In step 1,
499 ClairS uses Clair3 and LongPhase for germline variant calling, phasing and read haplotagging.
500 The processed alignments are then used for both pileup and full-alignment-based somatic
501 variant calling in step 2. Step 3 involves post-processing filters that eliminate somatic variant
502 calling if an ancestral haplotype (either maternal or paternal) from which the somatic variant
503 could originate cannot be found.

504

505 *Step 1: Germline variant calling, phasing and read haplotagging.* Step 1 is depicted in Figure 2b.
506 Clair3²² is integrated into ClairS for calling high-quality heterozygous germline variants in both
507 tumor and normal to maximize the performance of the subsequent phasing task. Unlike Clair3’s
508 default, AF \geq 0.2 and coverage \geq 10 were applied to ensure the quality of the called variants and
509 reduce computational overhead. Only the heterozygous germline variants found in both tumor

510 and normal were chosen for phasing. For phasing and haplotagging the tumor alignments, both
511 LongPhase³² and WhatsHap³³ are allowed in ClairS. We chose LongPhase over WhatsHap as the
512 default because LongPhase runs ~15 times faster while delivering similar or longer phase sets
513 on human samples. Notably, ClairS does not phase and haplotag the normal alignments. Our
514 experiment showed phasing the normal alignments doubled the processing time but did not
515 result in any improvement in calling performance.

516
517 *Step 2. Pileup-based and full-alignment-based variant calling.* Step 2 is depicted in Figure 2c. For
518 a variant candidate (explained in “Selecting variant candidates”), a pileup input and a full-
519 alignment input are generated (explained in “The design of pileup input and full-alignment
520 input”). Then the inputs are sent to a Bi-GRU-based pileup-calling neural network and a ResNet-
521 based full-alignment-calling neural network (explained in “The design of neural networks”) for
522 inference. Both networks have the same output – a single task with three categories, “Somatic”,
523 “Germline”, and “Artifact”, which match exactly the three categories defined in the synthetic
524 training data. In contrast to Clair3, in which the faster pileup-based calling cleans up most
525 variant candidates that are obvious variants, and the more computational-demanding full-
526 alignment-based calling handles the tricky and less obvious candidates, ClairS considers the
527 power of the two neural networks equal. We observed that full-alignment-based calling is
528 performant at mid-range VAFs. However, pileup-based calling requires less evidence than full-
529 alignment calling to draw the same conclusion. When VAF goes under 0.1, pileup-based calling
530 becomes increasingly more sensitive and usually outperforms full-alignment-based calling. This
531 observation makes pileup-based calling more important for somatic variant calling than its role
532 in Clair3 for germline variant calling, especially in multiple clinical usage scenarios when
533 sensitivity is emphasized. In ClairS, a somatic variant is called when both networks give somatic
534 the highest probability. The variant quality (QUAL) is Phred-like and is calculated as

535 $\max(-10\log_{10}\left(\frac{1-p}{p}\right) + 2, 0)$, where $p = \frac{P_{Somatic}^{Pileup} + P_{Somatic}^{Full-alignment}}{2}$. Also in contrast to Clair3,
536 which uses the same network for both SNP and Indel calling, ClairS uses two different networks
537 respectively trained for SNV and Indel calling. This means that ClairS runs on four networks in
538 total: pileup for SNV, pileup for Indel, full-alignment for SNV, and full-alignment for Indel. The
539 rationale behind the new design is that unlike germline variants that are commonly diploid,
540 somatic variants have no ploidy assumption, meaning that the existence of SNVs and Indels in
541 the same position are independent events. Our tests found that using separated networks led to
542 a 1.5% increase in SNV recall. The use of separated networks also allowed the use of different
543 variant quality cutoffs for SNV and Indel, which is useful for somatic variant calling, especially
544 when the sample condition is not ideal.

545
546 *Selecting variant candidates.* Sending every genome position as a variant candidate to the
547 neural networks guarantees maximum sensitivity. However, it is not only computationally
548 infeasible, but also unreasonable to work on nonstarter positions, such as those without any
549 non-reference allele support. A good variant candidate selection strategy is essential to achieve
550 a balance between sensitivity and running time. In ClairS, the selection criteria are as follows.
551 Let $r \in K = \{A, C, G, T\}$ be the reference base of a genome position, and $m \in K - r$ be the alternative
552 bases. D^X_m denotes the coverage of m at the position in sample $X \in \{T, N\}$, where T and N

553 represent the tumor and normal sample. C_m defines the selection criteria of each alternative
554 base in m , as:

$$555 \quad C_m = \begin{cases} \text{False} & \text{if } D_m^T < 3 \text{ or } \frac{D_m^T}{\sum_i^K D_i^T} < \alpha \\ \text{True} & \text{if } \frac{D_m^T}{\sum_i^K D_i^T} \geq \alpha \text{ and } \frac{D_m^N}{\sum_i^K D_i^N} < \alpha \\ \text{True} & \text{if } \frac{\frac{D_m^T}{\sum_i^K D_i^T}}{\frac{D_m^N}{\sum_i^K D_i^N}} \geq \beta \text{ and } \frac{D_m^N}{\sum_i^K D_i^N} \geq \alpha \end{cases}$$

556 where α sets the minimum VAF, and β sets the minimum tumor VAF to normal VAF ratio for a
557 candidate to be selected. Intuitively, the first equation means disregarding variant candidates
558 with < 3 reads in tumor supporting the variant allele, or with VAF in tumor $< \alpha$. The second
559 equation means selecting a variant candidate if its VAF is $< \alpha$ in normal, but $\geq \alpha$ in tumor. The
560 third equation means selecting a variant candidate, even if its VAF in normal is $\geq \alpha$, the VAF in
561 tumor is $\geq \beta$ times larger than the VAF in normal. In ClairS, α and β are configurable and default
562 to 0.05 and 6, respectively. Like model training data preparation, coverage ≥ 4 is required in both
563 tumor and normal for a candidate to be selected for variant calling.

564

565 *The design of pileup input and full-alignment input.* ClairS pileup input comprises 1,122 integers
566 – 33 positions wide with 34 features at each position (an example is given in Extended Data
567 Figure 2a). A detailed explanation of each feature is given in Supplementary Methods under
568 “Description of pileup input features”. ClairS has 18 pileup features in common with Clair3, and
569 16 additional features. The 16 new features are read counts N_{LMQ+} , N_{LMQ-} , N_{LBQ+} , and N_{LBQ-} ,
570 where N is either of the nucleotides A, C, G, and T, LMQ subscript means mapping quality lower
571 than 20 (MQ<20), LBQ means base quality lower than 30 (BQ<30), and + and - mean the
572 forward and reverse strand, respectively. The rationale behind the new features is that in ClairS,
573 the results of pileup-based calling and full-alignment-based calling are trusted equally, so the
574 mapping quality and base quality information that used to be exclusive to full-alignment calling
575 need to be added to pileup-based calling. Our experiment showed that removing the 16 new
576 features reduced precision by ~2% using 50x/25x of HCC1395/BL. ClairS full-alignment input
577 comprises 30,030 integers – seven channels, each with 33 positions and 130 rows to support at
578 most 76 tumor reads, 52 normal reads, and 2 empty rows as space between tumor and normal
579 (an example is given in Extended Data Figure 2b). Like Clair3, random subsampling down to the
580 maximum supported coverage is used at excessive coverages. A detailed explanation of each
581 channel is given in Supplementary Methods under “Description of full-alignment input
582 channels”. In both inputs, the candidate variant is centered at the 16th position. Positions
583 uncovered by any base in full-alignment input are filled with zero.

584

585 *Design of neural networks.* The pileup and full-alignment network architecture and important
586 parameters are shown in Figure 3. The pileup network uses two bidirectional gate recurrent unit
587 (Bi-GRU) layers, each with 128 and 192 units. Compared to the Clair3 pileup network, the use of
588 Bi-GRU instead of bidirectional long short-term memory (Bi-LSTM) architecture reduced
589 trainable parameters from 2,532,995 to 2,309,507 and matrix computations from 3.11 to 2.38

590 billion, but improved performance in our experiment. The full-alignment network is a residual
591 neural network (ResNet) comprising three standard residual blocks. A convolutional layer is
592 added immediately before each residual block to expand the number of channels. In both
593 networks, a dropout rate at 0.3 is set for the flattened layer and dense layer to prevent
594 overfitting.

595

596 *Step 3. Search for ancestral haplotype support.* Step 3 is depicted in Figure 2d. The neural
597 networks exhibited good power in distinguishing real variants from false positive candidates.
598 However, useful signals remote to a variant candidate are not covered by the current neural
599 network designs in ClairS, which considers only the flanking 16bp of a candidate. Notably, even
600 if the flanking window is extended to 50bp, it is still too short for an accurate inference of which
601 haplotype a variant candidate belongs to using only the networks, but the networks would
602 already be computationally infeasible for somatic variant calling. In ClairS, post-processing step
603 3 is designed to reduce false positive calling mistakes made by the networks by leveraging
604 relatively remote germline variants to find the correct ancestral haplotype for a somatic variant.
605 Any somatic variant calls that cannot be found with ancestral haplotype support are switched to
606 an artifact and are excluded from the output. The haplotagged reads produced in step 1 are
607 used in this step. For a somatic variant that covers any haplotagged reads, we required the
608 somatic variant to coexist with the heterozygous germline variants less than 100 bp away on its
609 left and right in the reads in the haplotype group the somatic variant supporting reads were in.
610 An example of a false positive somatic variant filtered by this rule is given in Extended Data
611 Figure 3a. A somatic variant at chr4:38,012,942 was called by the two networks. A phased
612 heterozygous germline variant was found 61 bp left of the somatic call. Three reads in haplotype
613 2 that supported the somatic variant were found not to have the heterozygous germline variant.
614 Thus, the somatic variant was considered unsupported by an ancestral haplotype. For a somatic
615 variant that covers no haplotagged read, it is probably because there are no germline variants
616 or only homozygous variants in the vicinity. In this case, we required the somatic variant to be
617 coexisting with the homozygous germline variants less than 100 bp away on its left and right in
618 all somatic variant supporting reads. An example of this is given in Extended Data Figure 3b. A
619 somatic variant at chr1:100,632,158 was called by the two networks. A homozygous germline
620 variant was found 39 bp left of the somatic call. Multiple reads that support the somatic variant
621 were found not to have the homozygous germline variant. Thus, the somatic variant was not
622 considered to be supported by an ancestral haplotype. Somatic variants that do not have any
623 germline variants less than 100 bp away on their left or right are not applicable in this step.

624

625 *Output.* ClairS supports VCF format output. Somatic variants are marked “PASS” or “LowQual” if
626 the variant quality is low (i.e., QUAL<8, configurable by option), or they are filtered in step 3. For
627 each variant, the allele frequency and supporting coverage of the reference allele and all
628 alternative alleles are shown. The options “--print_germline_calls” and “--print_ref_calls”
629 enable outputting germline variants and artifacts, respectively.

630

631 **ONT library preparation and sequencing**

632 Genomic DNA (gDNA) of a triple-negative breast cancer (TNBC) cell line (HCC1395) and a B
633 lymphocyte-derived normal cell line (HCC1395BL) from the same donor were purchased from
634 the American Type Culture Collection (ATCC). Genomic DNA (gDNA) of HG001 was purchased
635 from the Coriell Institute. The high-molecular-weight gDNA was examined by Nanodrop, Qubit,
636 and 0.35% agarose electrophoresis for its concentration, purity, and integrity. The gDNA was
637 then fragmented with gTube to generate DNA fragments approximately 20 kb in length. These
638 fragments were then being sequenced at two sequencing centers: HKU and Novogene. At HKU,
639 the fragments of HCC1395, HCC1395BL, and HG001 were prepared and ligated with a
640 sequencing adapter using ONT's ligation sequencing kit V14 SQK-LSK114. The ligated samples
641 were sequenced on R10.4.1 PromethION flowcells using a PromethION 2 Solo device and
642 MinKNOW software version 1.18.02, for 96 h. At Novogene, the fragments of HCC1395 and
643 HCC1395BL were prepared and ligated with a sequencing adapter using ONT's ligation
644 sequencing kit V12 SQK-LSK112. The ligated samples were sequenced on R10.4 PromethION
645 flowcells using PromethION 48, for 96 h.

646

647 **Benchmarking**

648 We used the truth set of somatic variants in HCC1395/BL generated and maintained by the
649 SEQC2 consortium. The truth set was orthogonally validated with multiple sequencing replicates
650 from multiple sequencing centers that comprise over 1,500-fold sequencing data in total. We
651 used only the somatic variants labeled "HighConf" (High Confidence) or "MedConf" (Medium
652 Confidence) as truth. Somatic variants labeled "LowConf" (Low Confidence, VAF \leq 0.05, not a
653 part of the truth set as defined by SEQC2) were not used for benchmarking. In total, there were
654 39,560 truth SNVs and 1,922 truth Indels; 39,447 of the SNVs and 1,602 of the Indels were
655 within the high-confidence regions defined in a BED file provided by SEQC2. A variant call was
656 considered correct only if it matched both the genome position and variant allele of the truth.
657 For both the ONT and Illumina benchmarks, some truth variants were excluded for the following
658 reasons. First, even with the high sequencing coverage, such as 75.97-fold HCC1395 we
659 generated for the ONT benchmarks, some truth variants still had very low or no coverage, or
660 had no read supporting the variant allele. These truth variants would fail all the benchmarks, so
661 they should be excluded. Second, some benchmarks tested multiple sequencing coverages and
662 required sequencing read subsampling from the full dataset. The subsampling process might
663 remove reads supporting a truth variant to an extent that few or no supporting reads are left.
664 This affects especially the somatic variants that already have a low VAF. For example, a VAF 0.05
665 somatic variant with 20-fold coverage and one read supporting the variant allele can be reduced
666 to VAF 0 by removing just one read during subsampling. This reduces the quality of the
667 benchmarking results, especially for low VAF truth variants when subsampled datasets are used.
668 To alleviate the problem, any truth variants that have very low VAF (<0.05) observed in the full
669 dataset before subsampling should be excluded. Summing up the two reasons above, for each
670 of the full datasets we used in both the ONT and Illumina benchmarks, we excluded truth
671 variants that matched any of the following criteria from benchmarking: 1) VAF \leq 0.05, 2) reads
672 supporting the variant allele <3 , 3) tumor coverage <4 , and 4) normal coverage <4 . For
673 standardization, we used som.py, provided in Illumina's Haplotype Comparison Tools²⁷ (version

674 v0.3.12) to generate evaluation metrics, including F1-Score, Precision, and Recall against the
675 truth variants. The “compare_vcf” submodule in ClairS produces identical results to som.py, but
676 automates the exclusion of unqualifying truth variants. The truth set materials are publicly
677 available to the community. All tools, their version, and command lines used are given in the
678 “Command lines used” section in Supplementary Notes.
679

680 Computational performance

681 ClairS was written in Python and C++. The Python parts leveraged PyPy for speed up. The neural
682 network implementations used PyTorch. Training ClairS neural networks requires a high-end
683 GPU, but using ClairS for somatic variant calling requires only a CPU. For the 50x/25x
684 HCC1395/BL pair, ClairS finished running in ~5 hours for ONT data and ~2 hours for Illumina data
685 (30% slower than Strelka2, but faster than all other short-read somatic variant callers), using
686 two 12-core Intel Xeon Silver 4116 processors. The memory footprint is low and is controlled at
687 lower than 1GB per CPU. For model training, we tested Nvidia GeForce RTX 2080 Ti, 3090, and
688 4090, and found each new model provided a ~35% speed increase from the previous
689 generation.
690
691

692 Code availability

693 ClairS is open source and available at <https://github.com/HKU-BAL/ClairS> under the BSD 3-
694 Clause license. The results in this paper were based on the ClairS initial release (version 0.0.1).
695 Multiple installation options are available for ClairS, including Docker and Singularity. ClairS has
696 also been included as the small variant caller in ONT’s somatic variant calling workflow²⁹ since
697 version 0.1.0.
698

699 Data availability

700 The links to the reference genomes, truth somatic variants, benchmarking materials, ONT, and
701 Illumina data are given in the “Data availability” section in Supplementary Notes. All analysis
702 output, including the VCFs and running logs, is available at
703 http://www.bio8.cs.hku.hk/clairs/analysis_result. The HCC1395/BL sequencing data generated
704 in this study was deposited in the NCBI short-read archive with accession ID PRJNA986292.
705

706 Acknowledgements

707 R.L. was supported by Hong Kong Research Grants Council grants GRF (17113721) and TRS (T21-
708 705/20-N), the Shenzhen Municipal Government General Program (JCYJ20210324134405015),
709 the URC fund from HKU, and Oxford Nanopore Technologies.
710

711 [Author contributions](#)

712 R.L. conceived the study. Z.Z. and R.L. designed the algorithms, implemented ClairS, and wrote
713 the paper. Y.L. and T.-W.L. evaluated the benchmarking results. All authors revised the
714 manuscript.

715

716 [Competing interests](#)

717 R.L. receives research funding from ONT. The other authors declare no competing interests.

718

719

720 References

- 721 1. Weinstein, J.N. et al. The cancer genome atlas pan-cancer analysis project. *Nature genetics* **45**, 1113-1120 (2013).
- 722 2. Perera-Bel, J. et al. From somatic variants towards precision oncology: evidence-driven reporting of treatment options in molecular tumor boards. *Genome medicine* **10**, 1-15 (2018).
- 723 3. Fang, L.T. et al. Establishing community reference samples, data and call sets for 724 benchmarking cancer mutation detection using whole-genome sequencing. *Nature 725 biotechnology* **39**, 1151-1160 (2021).
- 726 4. Krishnamachari, K. et al. Accurate somatic variant detection using weakly supervised 727 deep learning. *Nature Communications* **13**, 4248 (2022).
- 728 5. Sahraeian, S.M.E. et al. Deep convolutional neural networks for accurate somatic 729 mutation detection. *Nature communications* **10**, 1041 (2019).
- 730 6. Narzisi, G. et al. Genome-wide somatic variant calling using localized colored de Bruijn 731 graphs. *Communications biology* **1**, 20 (2018).
- 732 7. Fan, Y. et al. MuSE: accounting for tumor heterogeneity using a sample-specific error 733 model improves sensitivity and specificity in mutation calling from sequencing data. 734 *Genome biology* **17**, 1-11 (2016).
- 735 8. Cibulskis, K. et al. Sensitive detection of somatic point mutations in impure and 736 heterogeneous cancer samples. *Nature biotechnology* **31**, 213-219 (2013).
- 737 9. Larson, D.E. et al. SomaticSniper: identification of somatic point mutations in whole 738 genome sequencing data. *Bioinformatics* **28**, 311-317 (2012).
- 739 10. Kim, S. et al. Strelka2: fast and accurate calling of germline and somatic variants. *Nature 740 methods* **15**, 591-594 (2018).
- 741 11. Freed, D., Pan, R. & Aldana, R. TNscope: accurate detection of somatic mutations with 742 haplotype-based variant candidate detection and machine learning filtering. *biorxiv*, 743 250647 (2018).
- 744 12. Cooke, D.P., Wedge, D.C. & Lunter, G. A unified haplotype-based method for accurate 745 and comprehensive variant calling. *Nature biotechnology* **39**, 885-892 (2021).
- 746 13. Lai, Z. et al. VarDict: a novel and versatile variant caller for next-generation sequencing in 747 cancer research. *Nucleic acids research* **44**, e108-e108 (2016).
- 748 14. Kovaka, S., Ou, S., Jenike, K.M. & Schatz, M.C. Approaching complete genomes, 749 transcriptomes and epi-omes with accurate long-read sequencing. *Nature Methods* **20**, 750 12-16 (2023).
- 751 15. Ameur, A., Kloosterman, W.P. & Hestand, M.S. Single-molecule sequencing: towards 752 clinical applications. *Trends in biotechnology* **37**, 72-85 (2019).
- 753 16. Nanopore Q20+ chemistry, <https://nanoporetech.com/q20plus-chemistry>. (2019).
- 754 17. Fox, E.J., Reid-Bayliss, K.S., Emond, M.J. & Loeb, L.A. Accuracy of next generation 755 sequencing platforms. *Next generation, sequencing & applications* **1** (2014).
- 756 18. Luo, R., Sedlazeck, F.J., Lam, T.-W. & Schatz, M.C. A multi-task convolutional deep neural 757 network for variant calling in single molecule sequencing. *Nature communications* **10**, 758 998 (2019).

762 19. Poplin, R. et al. A universal SNP and small-indel variant caller using deep neural
763 networks. *Nature biotechnology* **36**, 983-987 (2018).

764 20. Wagner, J. et al. Benchmarking challenging small variants with linked and long reads. *Cell*
765 *Genomics* **2**, 100128 (2022).

766 21. Luo, R. et al. Exploring the limit of using a deep neural network on pileup data for
767 germline variant calling. *Nature Machine Intelligence* **2**, 220-227 (2020).

768 22. Zheng, Z. et al. Symphonizing pileup and full-alignment for deep learning-based long-
769 read variant calling. *Nature Computational Science* **2**, 797-803 (2022).

770 23. Shafin, K. et al. Haplotype-aware variant calling with PEPPER-Margin-DeepVariant
771 enables high accuracy in nanopore long-reads. *Nature methods* **18**, 1322-1332 (2021).

772 24. Smolka, M. et al. Comprehensive structural variant detection: from mosaic to
773 population-level. *BioRxiv*, 2022.2004. 2004.487055 (2022).

774 25. Shiraishi, Y. et al. Precise characterization of somatic complex structural variations from
775 tumor/control paired long-read sequencing data with nanomonsv. *Nucleic Acids*
776 *Research*, gkad526 (2023).

777 26. Ewing, A.D. et al. Combining tumor genome simulation with crowdsourcing to
778 benchmark somatic single-nucleotide-variant detection. *Nature methods* **12**, 623-630
779 (2015).

780 27. Krusche, P. et al. Best practices for benchmarking germline small-variant calls in human
781 genomes. *Nature biotechnology* **37**, 555-560 (2019).

782 28. Shiraishi, Y. et al. Precise characterization of somatic complex structural variations from
783 paired long-read sequencing data with nanomonsv. *BioRxiv*, 2020.2007. 2022.214262
784 (2020).

785 29. Nanopore EPI2ME Labs, <https://github.com/epi2me-labs/wf-somatic-variation>. (2023).

786 30. Sahraeian, S.M.E. et al. Achieving robust somatic mutation detection with deep learning
787 models derived from reference data sets of a cancer sample. *Genome Biology* **23**, 12
788 (2022).

789 31. Tarabichi, M. et al. A practical guide to cancer subclonal reconstruction from DNA
790 sequencing. *Nature methods* **18**, 144-155 (2021).

791 32. Lin, J.-H., Chen, L.-C., Yu, S.-C. & Huang, Y.-T. LongPhase: an ultra-fast chromosome-scale
792 phasing algorithm for small and large variants. *Bioinformatics* **38**, 1816-1822 (2022).

793 33. Patterson, M. et al. WhatsHap: weighted haplotype assembly for future-generation
794 sequencing reads. *Journal of Computational Biology* **22**, 498-509 (2015).

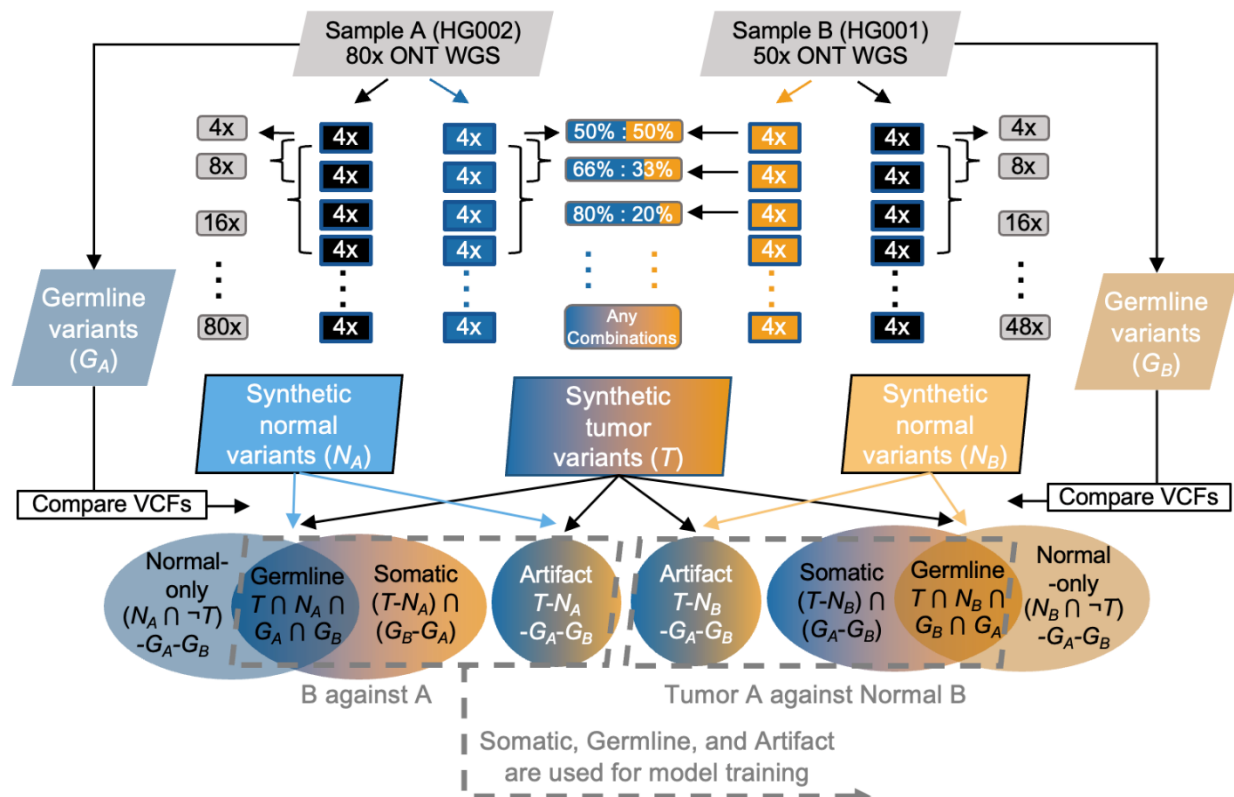
795

796

797 Figures

798

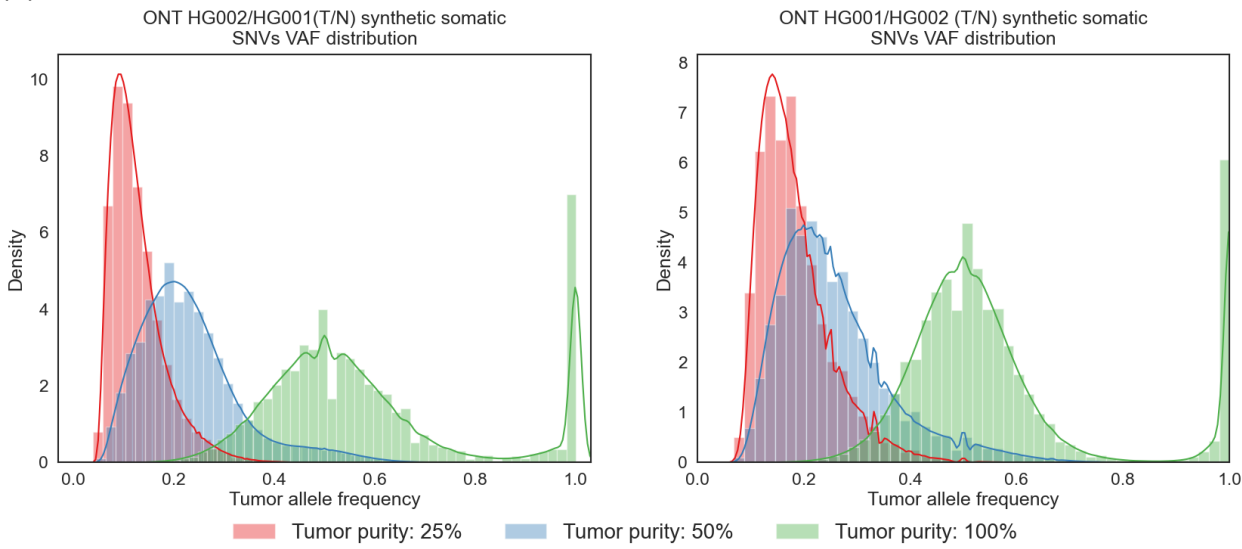
799 (a)



800

801

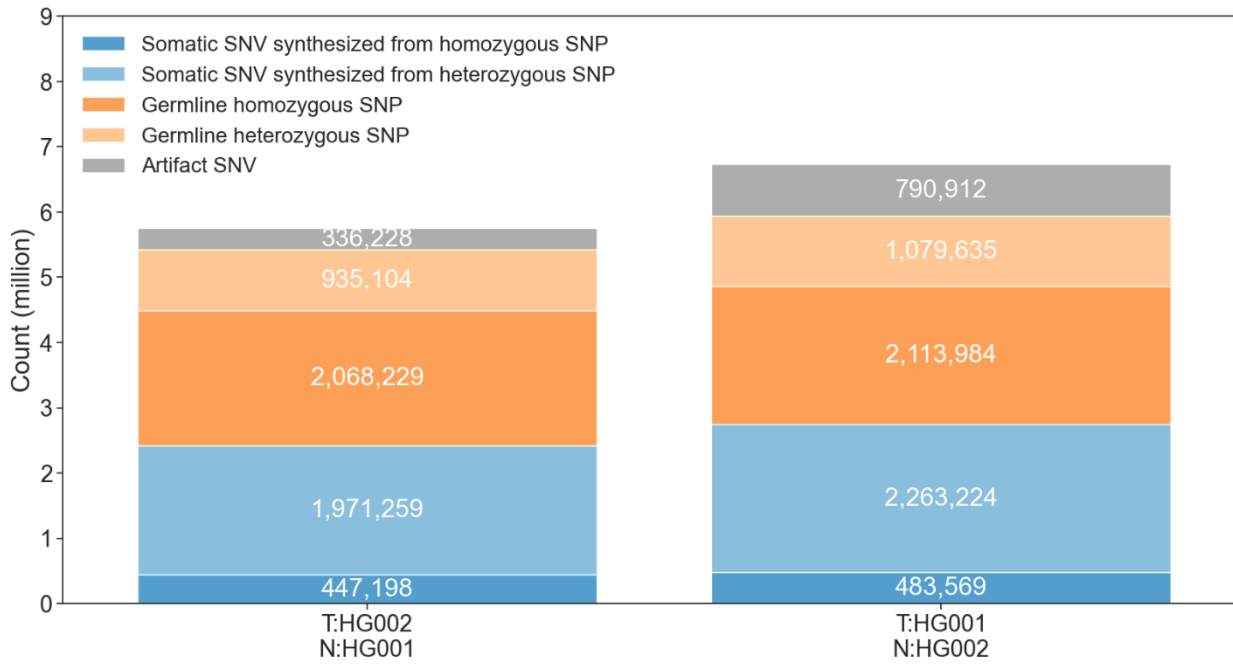
802 (b)



803

804

805 (c)



806
807

808 **Figure 1. Overview of ClairS training data synthesis workflow.**

809 (a) The workflow demonstrates how to produce synthetic somatic variants using two biologically
810 unrelated samples with known truth germline variants for ClairS model training. In this study,
811 specifically, we used 80x ONT WGS data of GIAB HG002 as sample A, and 50x HG001 as sample
812 B. First, germline variants G_A and G_B were defined as known truth germline variants in sample A
813 and B given by GIAB. G_A and G_B include both homozygous and heterozygous germline variants of
814 a sample. To generate synthetic tumor variants T and synthetic normal variants N_A/N_B for each
815 sample, the alignments were split into smaller chunks with 4x coverage each. Then, the chunks
816 from both samples were combined and the variants called from them were defined as T . With
817 the flexibility of combining any number of chunks from both samples, T effectively covered
818 variants called at different coverages and VAF. Similarly, the chunks from a sample were
819 combined at multiple coverages for calling synthetic normal variants N_A and N_B . With a small
820 number of chunks from another sample combined into a synthetic normal, N_A and N_B effectively
821 covered different contamination levels. The variants G_A , G_B , T , N_A and N_B were then used to
822 generate four categories of variants – “Somatic”, “Germline”, “Artifact”, and “Normal-only” –
823 with different rules. Somatic, Germline, and Artifact match the three categories in the inference
824 task of the ClairS network architecture. The variants of the three categories were used for
825 model training. When using sample B as tumor and A as normal, Somatic is defined as “ $(T-N_A) \cap$
826 (G_B-G_A) ”, i.e., variants that were 1) found in synthetic tumor T ; 2) not found in synthetic normal
827 N_A ; 3) found as a germline variant in G_B ; or 4) not found in G_A . Germline is defined as “ $T \cap N_A \cap$
828 $G_A \cap G_B$ ”, i.e., variants that were found in all T , N_A , G_A , and G_B . Artifact is defined as “ $T-N_A-G_A-G_B$ ”,
829 which signifies the variants found only in T and not in the germlines or synthetic normal.
830 When using sample A as tumor and B as normal, the definitions remain the same except for
831 switching the subscripts.

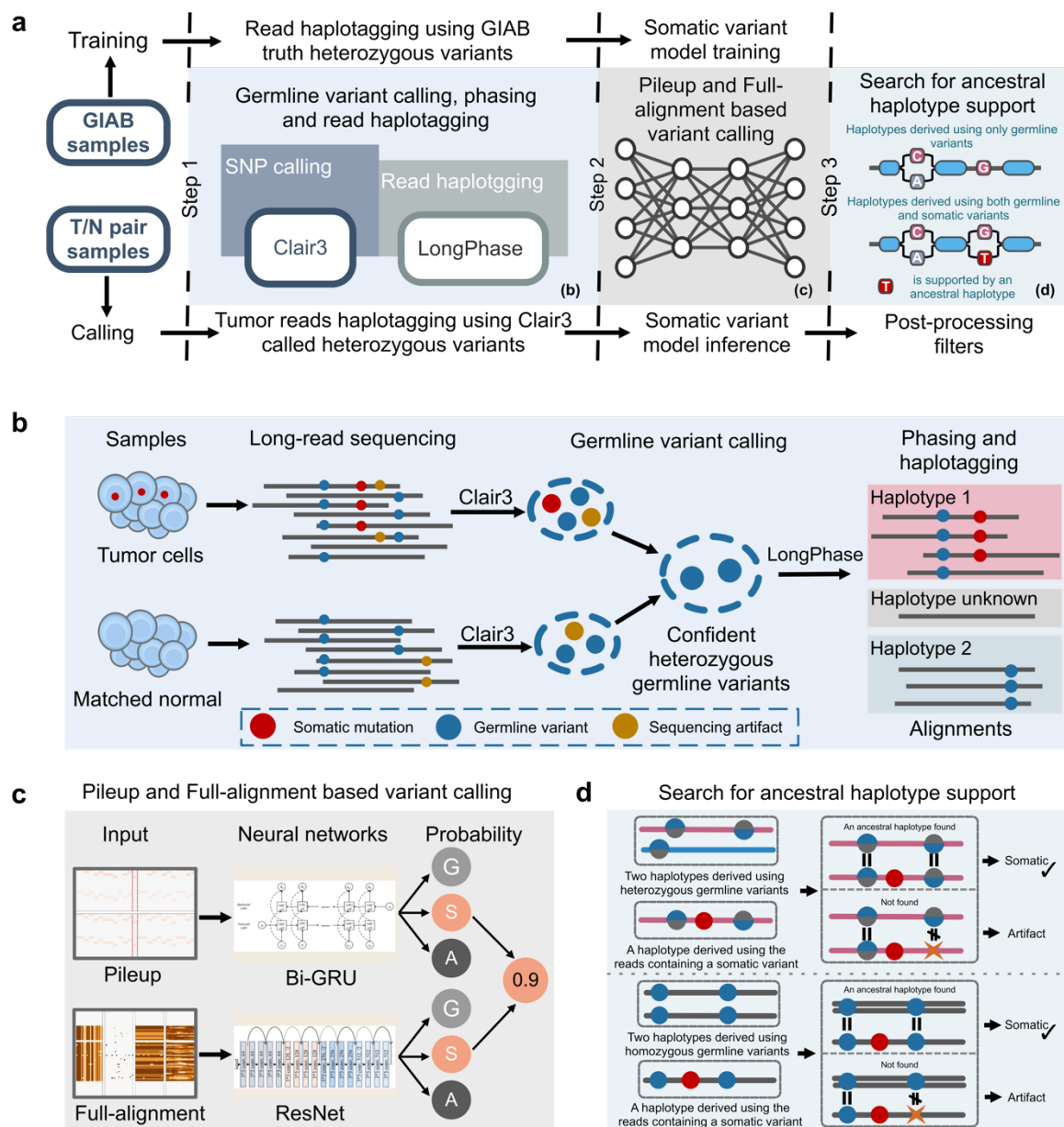
832 (b) The VAF distribution of the synthetic somatic SNVs at three different simulated tumor
833 purities (100%, 50%, and 25%), using either HG001/HG002 or HG002/HG001 as tumor/normal.
834 Since both heterozygous and homozygous variants were used in synthesis, at 100% tumor
835 purity, the variants were gathered at 0.5 and 1.0 VAF. The distribution showed good coverage of
836 typical somatic SNV VAF by the synthetic SNVs.

837

838 (c) The breakdown of the number of synthetic variants for training. The numbers 1) using either
839 HG002/HG001 or HG001/HG002 as tumor/normal, and 2) of the three categories Somatic,
840 Germline, and Artifact, as defined in subfigure a, are shown. The number of Somatic categories
841 is further divided into those synthesized from either homozygous SNPs or heterozygous SNPs.
842 These numbers explain why including heterozygous SNPs in the synthesis is essential to ensure a
843 sufficient number of synthetic somatic variants for model training.

844

845



846
847

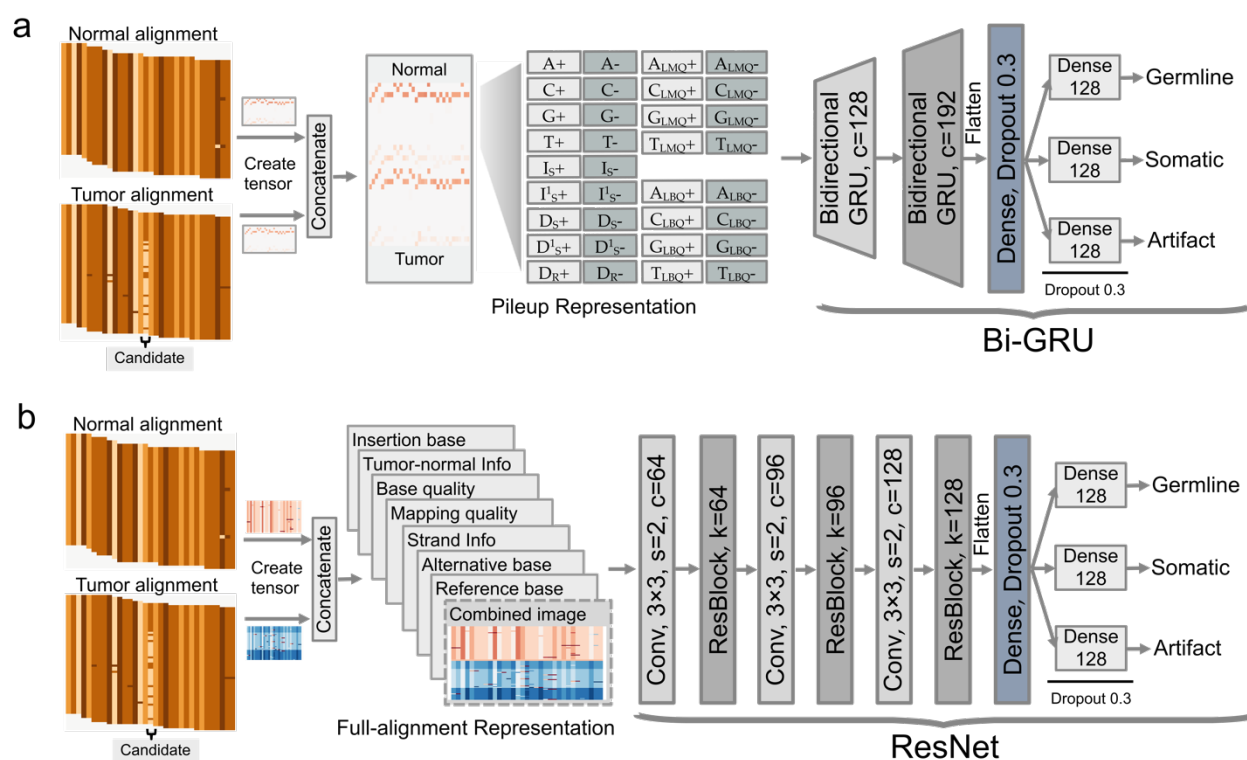
848 **Figure 2. Overview of the ClairS somatic variant calling workflow.**

849 (a) The workflow illustrates the three steps of ClairS. In step 1, ClairS uses Clair3 and LongPhase
850 for germline variant calling, phasing and read haplotagging. The processed alignments are then
851 used for both pileup- and full-alignment-based somatic variant calling in step 2. Step 3 involves
852 post-processing filters that eliminate somatic variant callings if an ancestral haplotype (maternal
853 or paternal) from which the somatic variant could originate cannot be found. The details of
854 steps 1, 2, and 3 are shown in subfigures b, c, and d. (b) Step 1 details. Clair3 is applied to both
855 tumor and normal samples for germline variant calling. High-quality heterozygous germline
856 variants shared by both samples are selected and used by LongPhase to phase the germline
857 variants found in the tumor sample. Using the phased germline variants, the tumor reads are

858 then haplotagged to belong to either haplotype 1, 2, or unknown. (c) Step 2 details. The
859 processed alignments from step 1 are fed into both the pileup-based variant-calling neural
860 network and the full-alignment based variant-calling neural network. On a single somatic variant
861 candidate, both networks give respective predictions on the probability of three categories:
862 “Somatic”, “Germline”, and “Artifact”. The predictions are then merged according to a set of
863 rules introduced in the Method section. (d) Step 3 details. The somatic variants called in step 2
864 are examined to determine if they are supported by an ancestral haplotype. Ancestral
865 haplotypes, which can be either maternal or paternal, are derived using germline variants. A
866 somatic variant is considered supported by an ancestral haplotype if the haplotype containing
867 the somatic variant is believed to originate from one of the ancestral haplotypes.

868

869



870

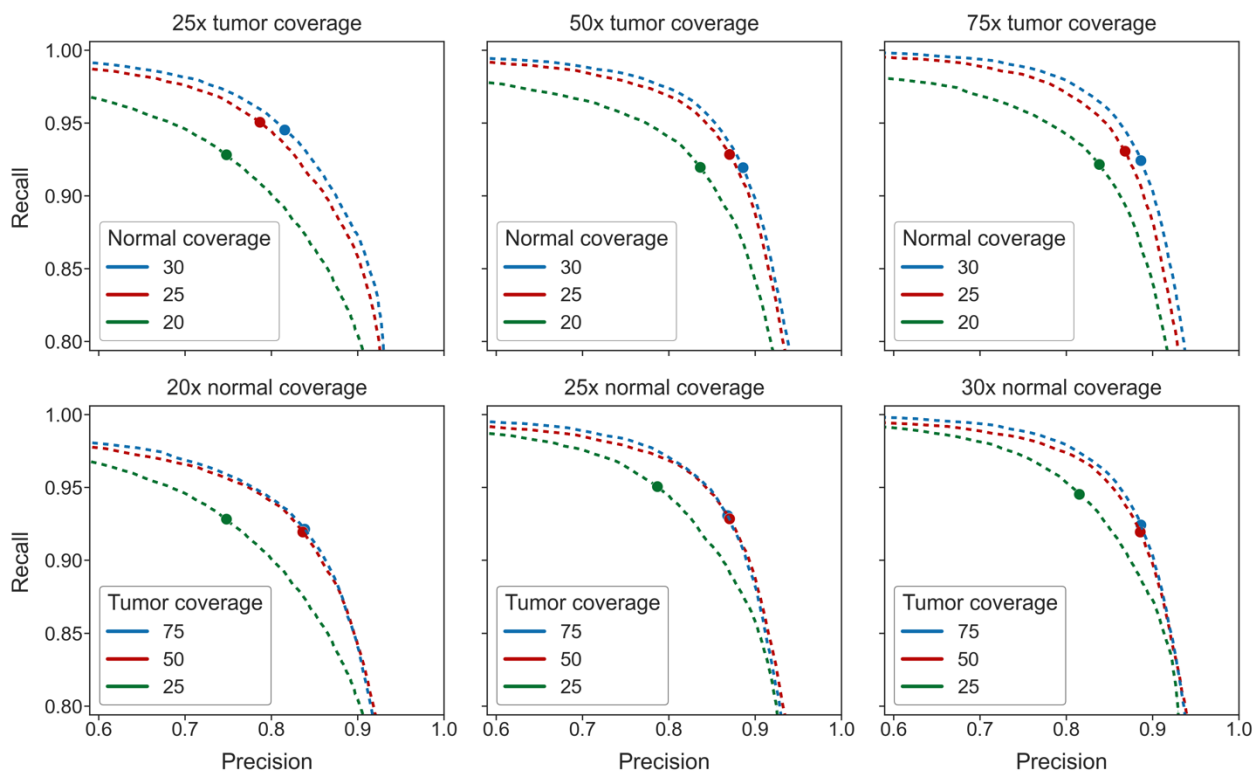
871

872 **Figure 3. The ClairS neural network architecture.**

873 Both (a) the pileup network and (b) full-alignment network use alignments of both the tumor
874 and normal samples as input. Tensors are created from both samples using methods detailed in
875 the Method section, and are then concatenated. The tensors are then processed by their
876 respective neural network for inference. Both networks output the probability of three
877 categories: “Germline”, “Somatic”, and “Artifact”. The sequence of layers and layer
878 configurations are shown. The letters c, s, and k, represent channel, stride, and kernel,
879 respectively.

880

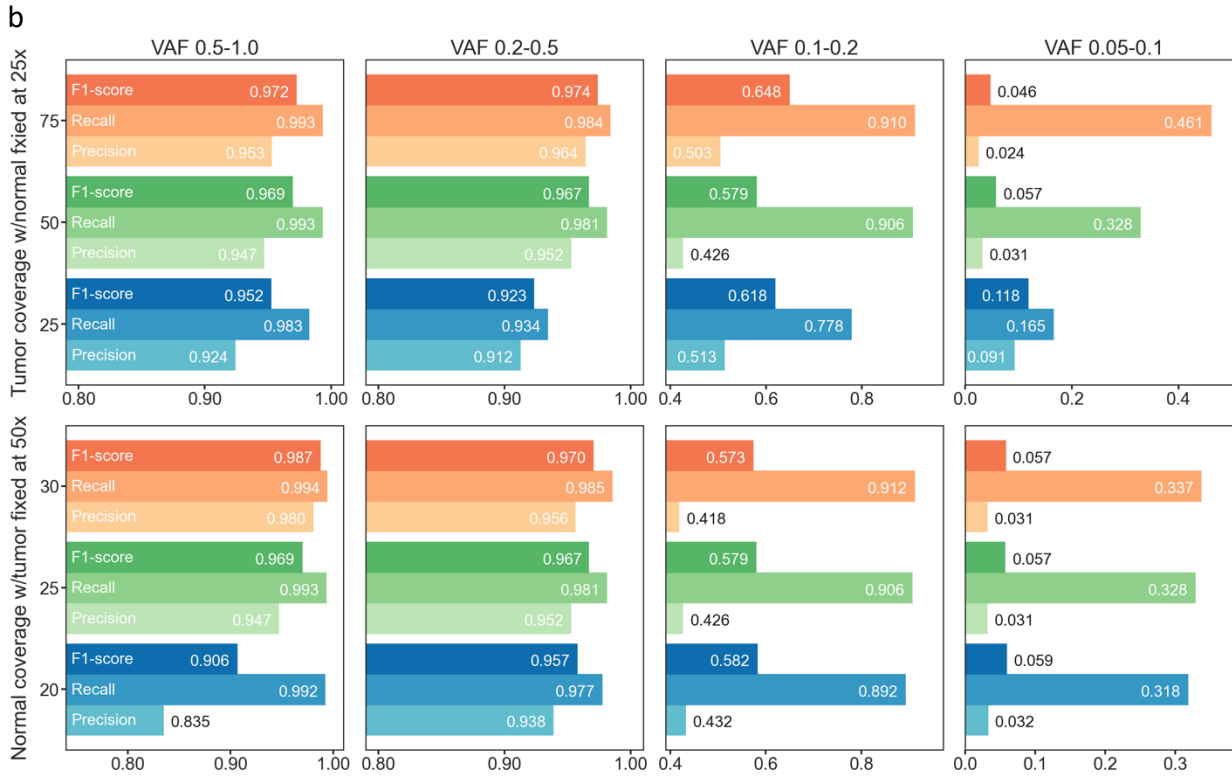
881 a



882

883

884



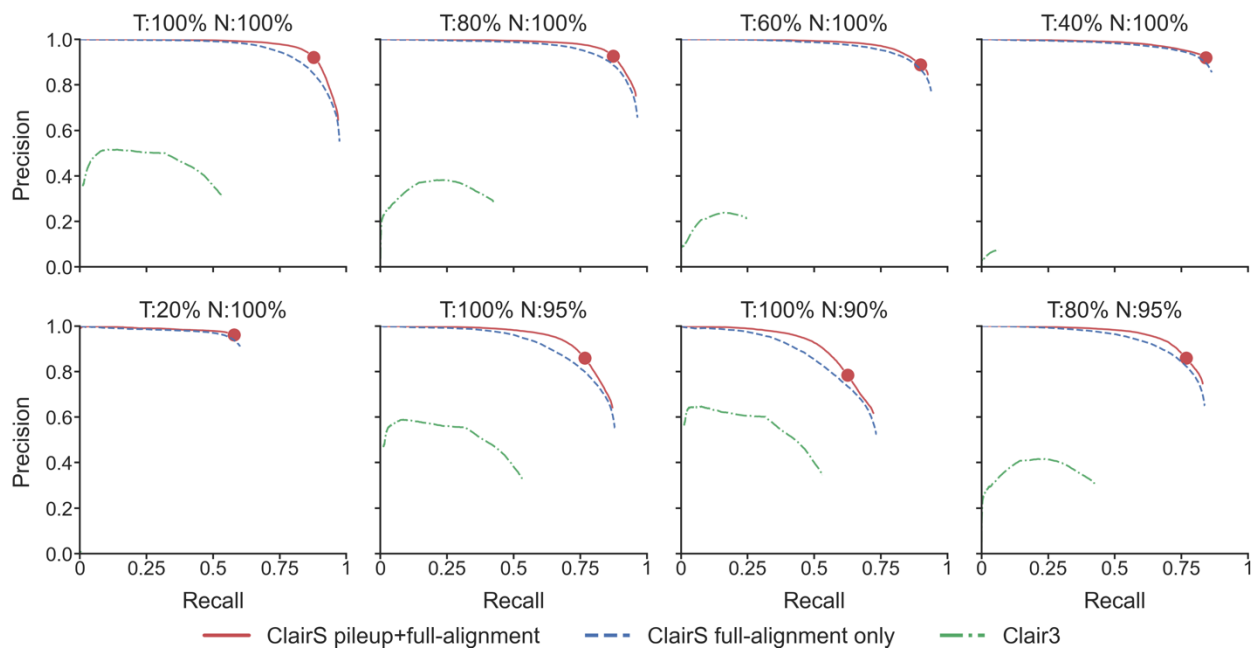
885

886

887

888

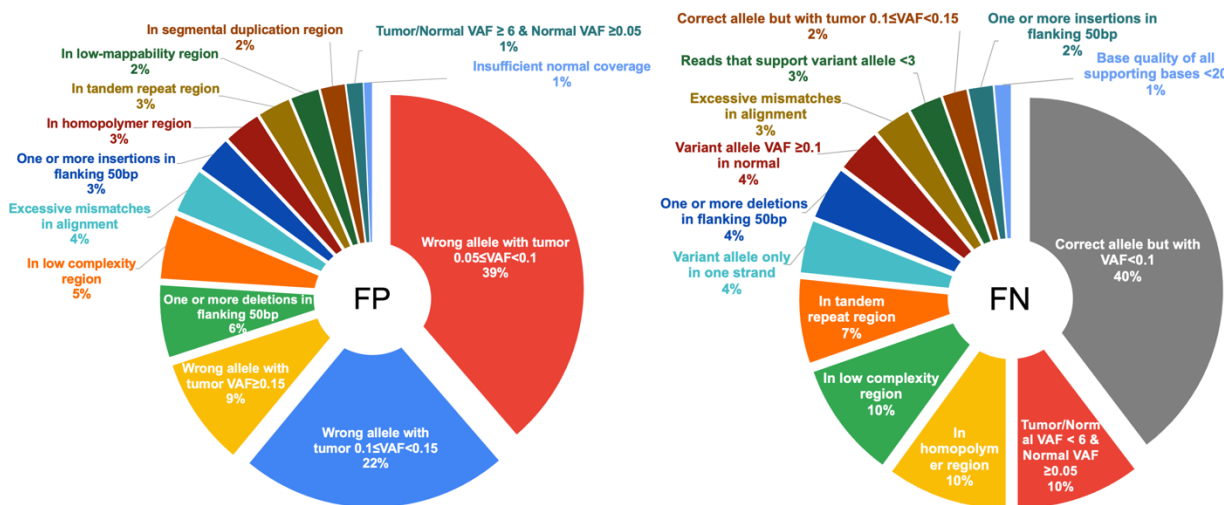
c



889
890

891 **Figure 4. ONT HCC1395/BL dataset benchmarking results.**

892 (a) The precision-recall curve of different combinations of tumor and normal coverage. The dot
893 on each dashed line shows where the best F1-score was achieved. (b) The performance of ClairS
894 at multiple VAF ranges benchmarked on the ONT HCC1395/BL dataset. In the first row, 25, 50x,
895 and 75x tumor were tested, with the normal coverage fixed at 25x. In the second row, 20x, 25x,
896 and 30x of normal were tested, with tumor coverage fixed at 50x. Variant quality cutoff 8
897 (prioritize-recall mode) was used. (c) The precision-recall curve of different tumor/normal purity
898 combinations with tumor coverage fixed at 50x and normal coverage fixed at 25x.
899
900

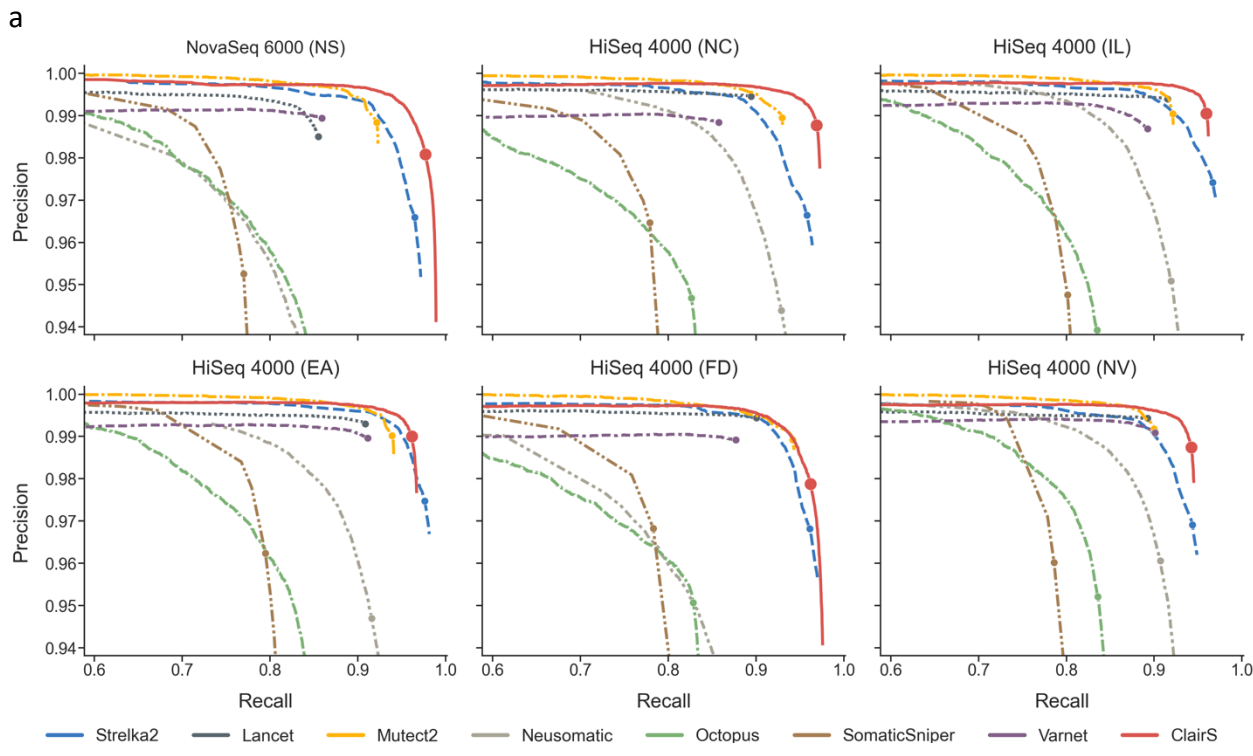


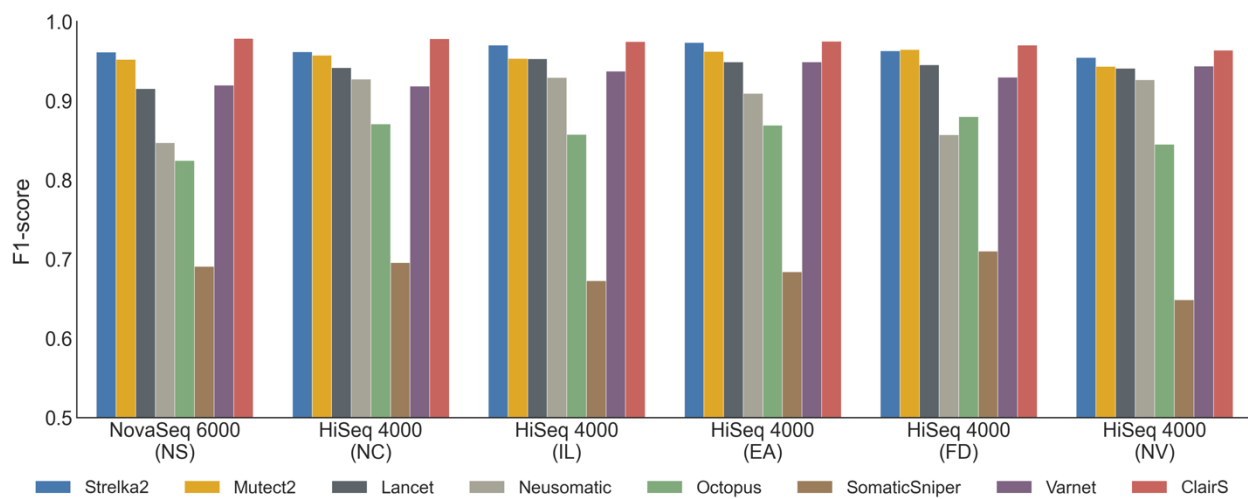
901
902

903 **Figure 5. Categorizing the FPs and FNs in ClairS**

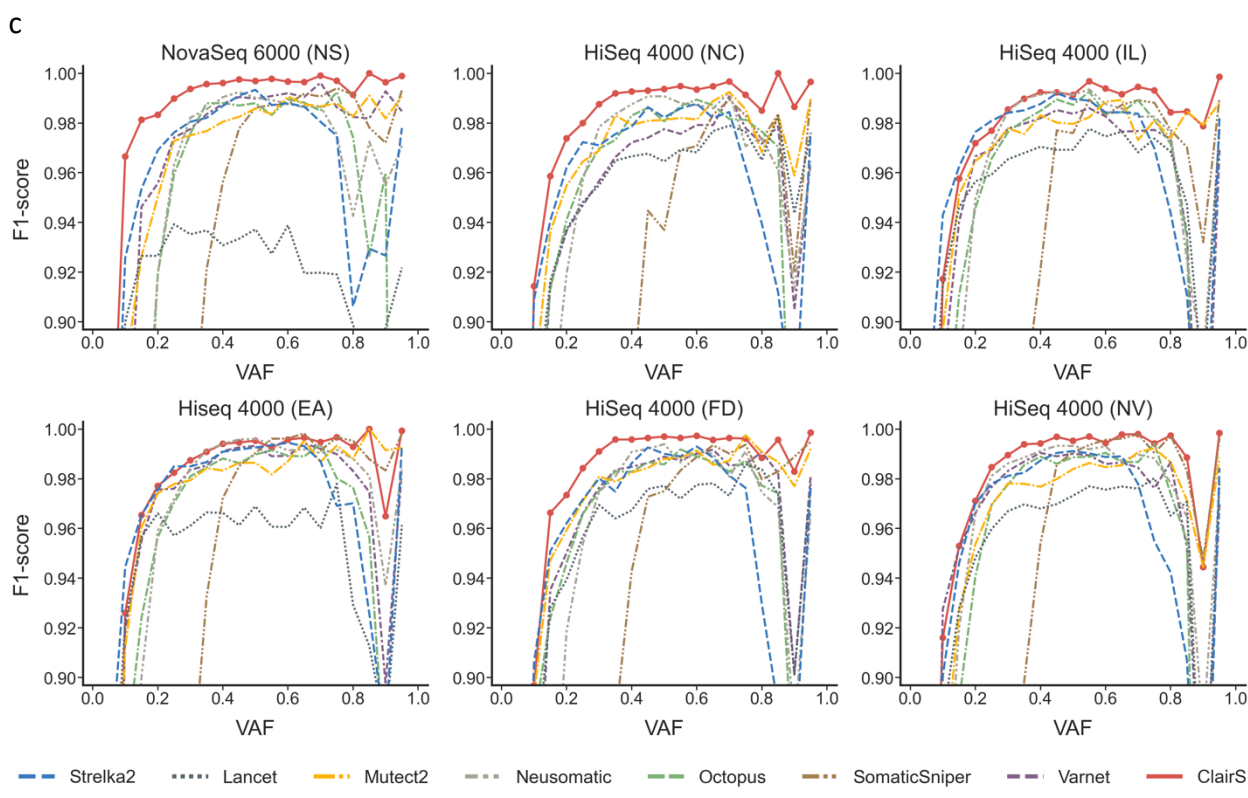
904 The pie charts show the distribution of reasons for the FPs and FNs in ClairS. A 50x/25x ONT
905 HCC1395/BL dataset was used for calling. 300 FPs and 300 FNs were randomly chosen from the
906 results and analyzed. The tandem repeat, low complexity, homopolymer, and segmental
907 duplication regions were defined using GIAB v3.0 Genome Stratification. Among the categories,
908 “excessive mismatches in alignment” and “insufficient normal coverage” were decided
909 manually, i.e., without certain cut-offs. “Excessive mismatches in alignment” was given if an eye
910 check of the alignments revealed excessive inconsistent mismatches than usual alignments with
911 a true somatic variant. “Insufficient normal coverage” was given when a germline variant signal
912 existed in both tumor and normal, but the coverage of normal was low, so the germline variant
913 signal in normal was obviously weaker than in tumor.

914
915
916



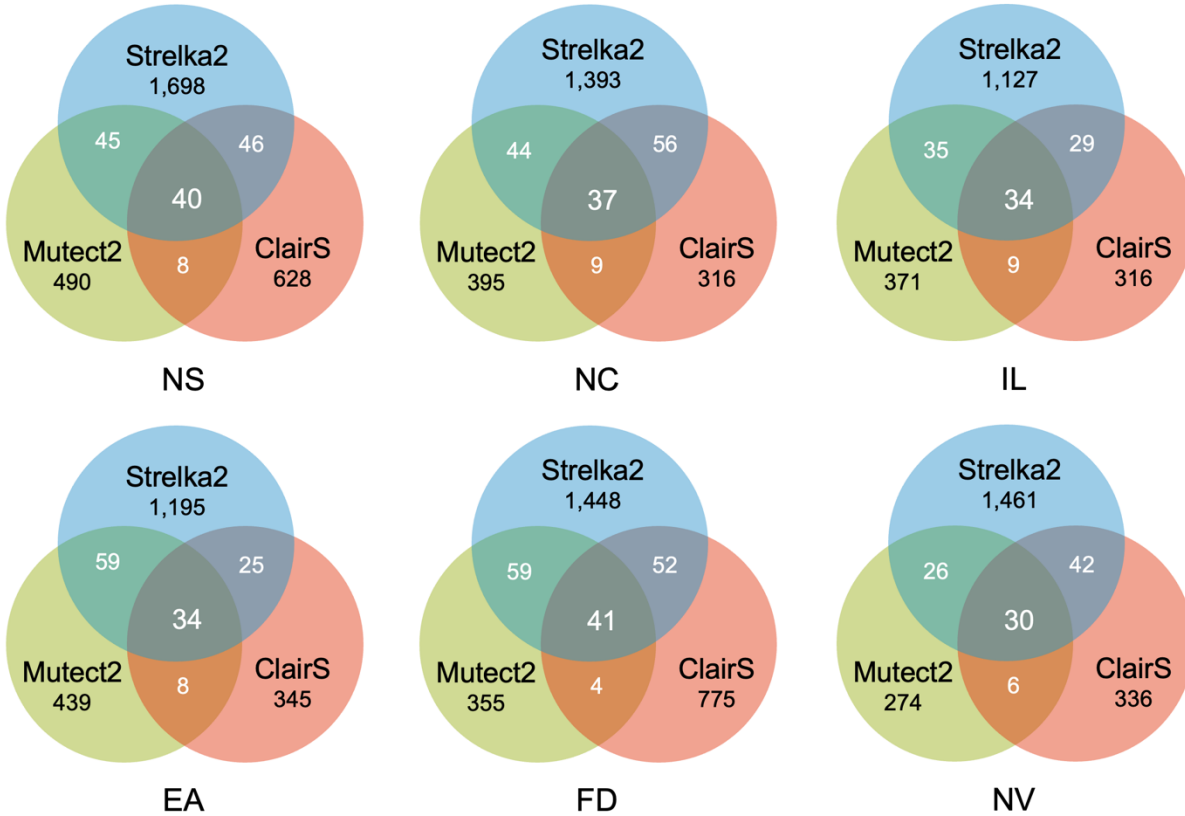


920
921
922



923
924
925

d



926
927

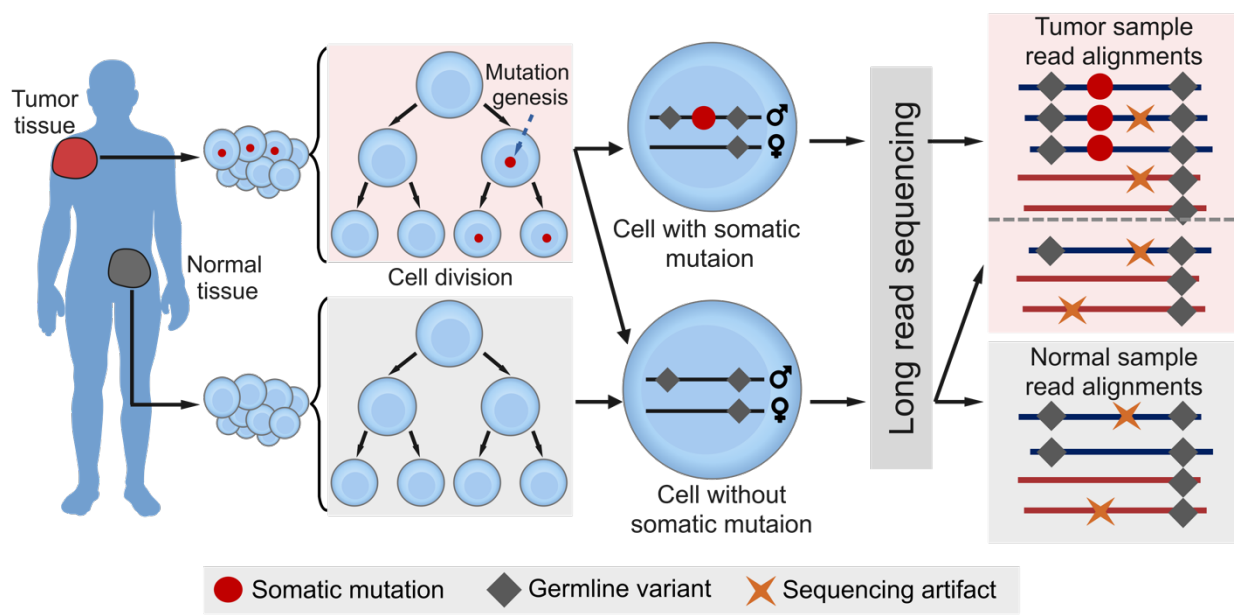
928 **Figure 6. Ilumina HCC1395/BL dataset benchmarking results.**

929 (a) The precision-recall curve of HCC1395/BL short-read datasets from six SEQC2 sources (NS:
930 NovaSeq at Illumina, NC: HiSeq at National Cancer Institute, IL: HiSeq at Ilumina, EA: HiSeq at
931 European Infrastructure for Translational Medicine, FD: HiSeq at Fudan University, NV: HiSeq at
932 Novartis) using eight tools (Strelka2, Lancet, Mutect2, Neusomatic, Octopus, SomaticSniper,
933 Varnet, ClairS). Variants were ranked by Strelka2 – SomaticEVS, Mutect2 – TLOD, VarNet – Score,
934 SomaticSniper – SSC, and other callers – QUAL. The dot on each line shows where the best F1-
935 score was. (b) The overall F1-score of the experiments shown in subfigure a. (c) The F1-score at
936 different VAFs of the experiments shown in subfigure a. (d) Venn diagrams showing the overlap
937 of false positive variant calls between Strelka2, Mutect2, and ClairS.

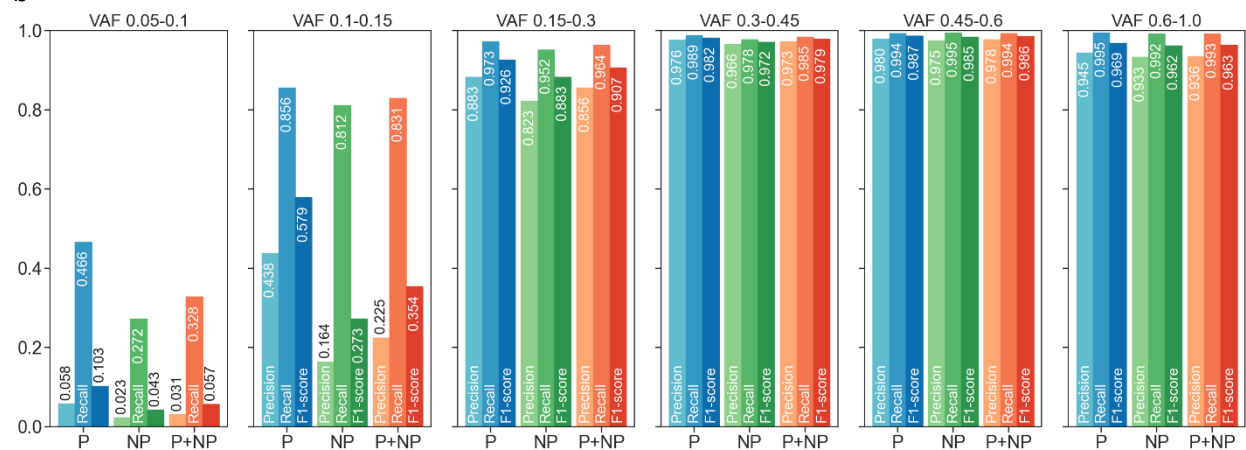
938
939

940 Extended Data Figures

941 a



942
943
944 b



945
946

947 Extended Data Figure 1. Performance differences between phasable and not-phasable
948 SNVs

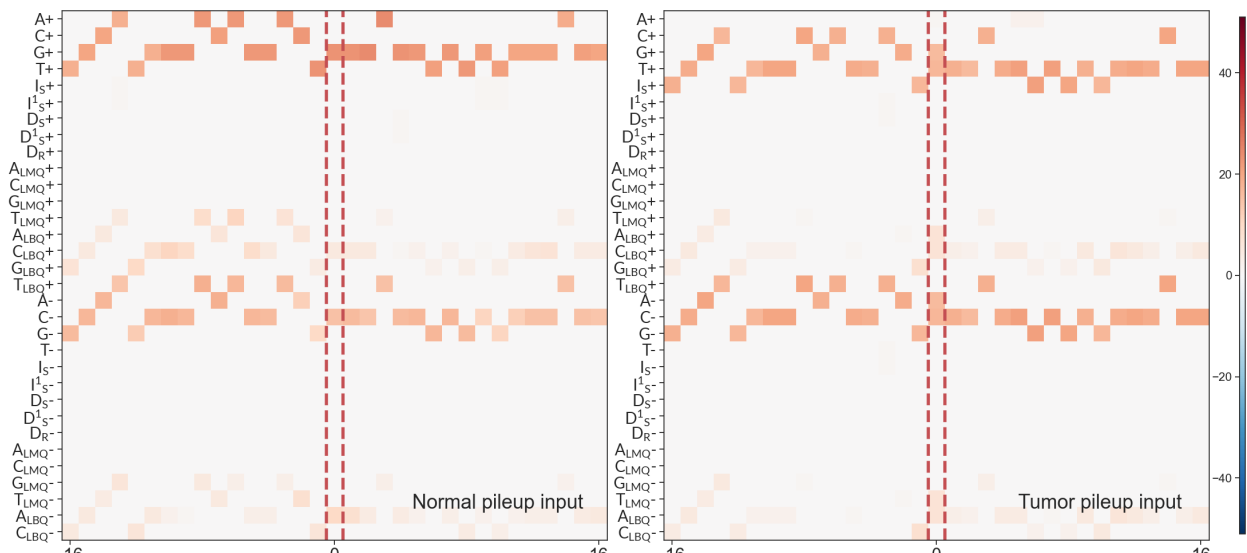
949 (a) The figure shows that a somatic variant usually originates in a single somatic cell and then
950 spreads to more cells through cell division, resulting in a clonal carrying the same variant. It also
951 shows how the mismatches in the tumor sample and normal sample are different from each
952 other. A somatic variant is more likely to be assigned to a haplotype through phasing, while a
953 variant caused by random sequencing errors is less likely to be successfully phased. (b) A
954 performance comparison of somatic variants where "P": can be phased, and "NP": cannot. The

955 figure shows a higher performance in somatic variants that can be phased, especially at lower
956 VAFs. We used 50/25-fold HCC1395/BL and prioritize-recall mode.

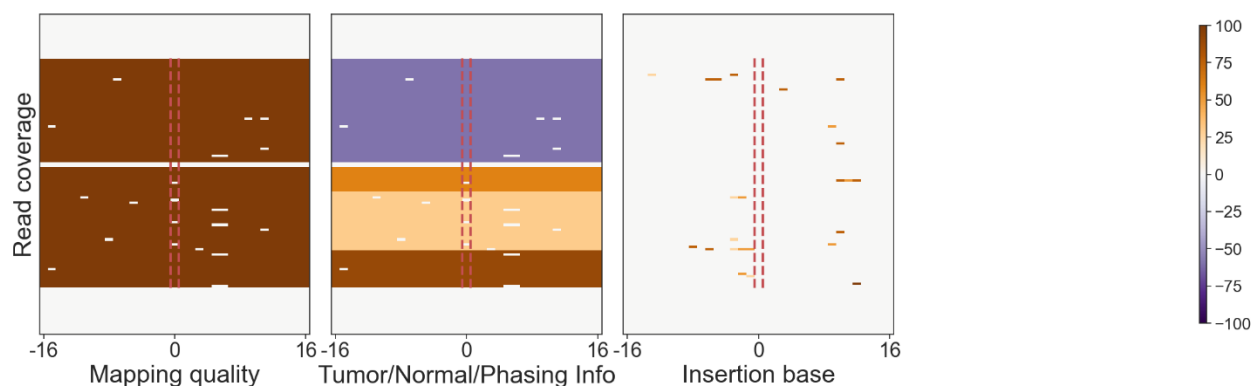
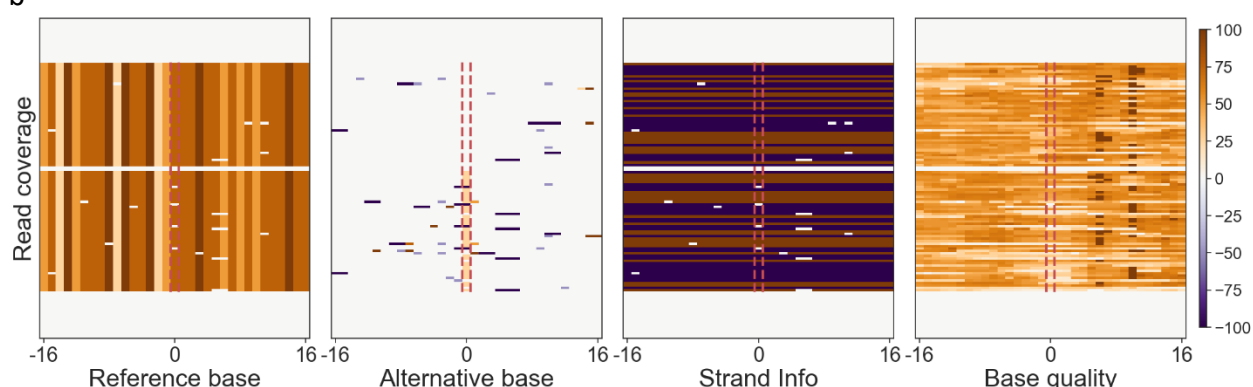
957

958

959 a



b



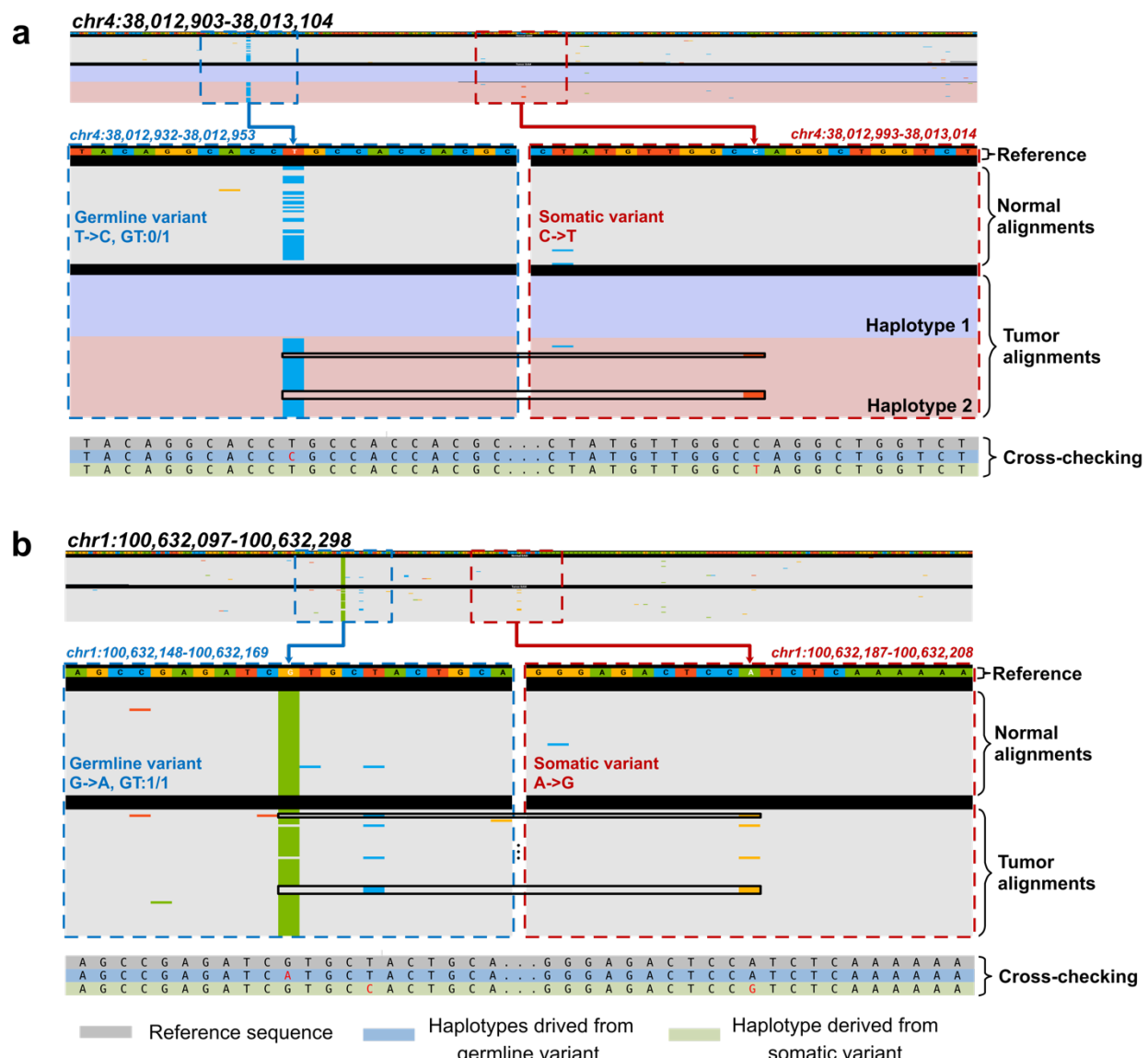
962

963

964 **Extended Data Figure 2. Visualization of neural network inputs.**

965 (a) Pileup-based calling input visualization. The candidate site is centered and marked by two
966 dashed lines. (b) Full-alignment-based calling input visualization. In b, the top and bottom are
967 padded with zero when the total coverage of tumor and normal samples does not reach the
968 input limit. The normal read alignments and tumor read alignments in all channels are
969 separated by two rows filled with zeros. The two demonstrations involved truth variants
970 randomly picked from the HCC1395/BL dataset.

971
972



973
974

975 **Extended Data Figure 3. Two examples of haplotype inconsistency that signifies a false**
976 **somatic call.**

977 (a) Example of a false somatic call with a haplotype inconsistent with the haplotype derived
978 from a heterozygous germline variant nearby. (b) Example of a false somatic call with a
979 haplotype inconsistent with the haplotypes derived from a homozygous germline variant
980 nearby. The bases A, C, G, and T are depicted in green, blue, yellow, and red, respectively. The
981 background in gray, purple, and pink represents an unknown haplotype, haplotype 1, and
982 haplotype 2, respectively. GT is an abbreviation of genotype.

983

984